

DYNAMIC RESPONSE OF CANTILEVER HIGHWAY SIGN STRUCTURES

SUBJECTED TO GUST LOADINGS

APPROVED:

To my wife Pam, for her understanding
and support

DYNAMIC RESPONSE OF CANTILEVER HIGHWAY SIGN STRUCTURES

SUBJECTED TO GUST LOADINGS

by

NICOLAS STEVEN COCAVESSIS, B.S.

THESIS

Presented to the Faculty of the Graduate School of

The University of Texas at Austin

in Partial Fulfillment

of the Requirements

for the Degree of

MASTER OF SCIENCE IN ENGINEERING

THE UNIVERSITY OF TEXAS AT AUSTIN

May 1978

A B S T R A C T

This study investigated the dynamic response of two cantilever highway sign structures subjected to truck-induced gust loadings. Both experimental and analytical procedures were used. The dynamic characteristics found by both procedures were in close agreement. The damping ratios for both signs were very low and resulted in a large number of stress cycles. The gusts caused by box-type trucks produced the highest measured response in the signs, whereas ambient wind response was generally negligible. An impulse-loading function was developed to simulate truck-induced gust loads and produced results in close agreement with the experimental results. Superstructure stresses are low and present no fatigue problems. Anchor bolt stress ranges were calculated and a simple fatigue analysis was presented.

A C K N O W L E D G M E N T S

The results herein represent one phase of the research study, Fatigue Loading on Sign Structures, sponsored jointly by the Texas State Department of Highways and Public Transportation and the Federal Highway Administration under an agreement with The University of Texas at Austin and the Texas State Department of Highways and Public Transportation.

The author expresses his gratitude to Dr. Karl H. Frank, principal investigator of the study and supervisor of the thesis, for the invaluable advice and support offered throughout the author's stay at The University of Texas at Austin. The encouragement and assistance of Dr. Richard E. Klingner is gratefully acknowledged. Special thanks are offered to Gorham W. Hinckley and Bruce M. Creamer for the help provided during the field study. Appreciation is extended to Jerry D. Crane, L. David Marschall, Daniel Perez, and J. Thomas Phillips for their expertise in instrumentation techniques and maintenance of field equipment. Assistance provided on the SAP IV computer program by Atalay Yargicoglu is acknowledged. Michael R. Lumsden is due credit for the drafting of figures. Thanks are expressed to all other staff members of the Civil Engineering Structures Research Laboratory who helped during the study, and in particular to Mrs. Maxine R. DeButts for her advice and expertise in typing the complete thesis.

N. S. C.

February 1978
Austin, Texas

C O N T E N T S

Chapter		Page
1	INTRODUCTION	1
	1.1 Objectives	1
	1.1.1 Dynamic Response	1
	1.2 Experimental Program	4
	1.3 Analytical Program	4
2	EXPERIMENTAL PROCEDURE	6
	2.1 Sign Selection	6
	2.2 Instrumentation	9
	2.2.1 Strain Gages	9
	2.2.2 Wind-sensing Equipment	13
	2.2.3 Recording Equipment	13
	2.2.4 Power Supply	15
	2.3 Data Accumulation	15
3	EXPERIMENTAL RESULTS	18
	3.1 Double Cantilever	18
	3.1.1 Dynamic Characteristics	21
	3.1.2 Truck-induced Data	25
	3.1.3 Ambient Wind Data	30
	3.2 Single Cantilever	33
	3.2.1 Dynamic Characteristics	33
	3.2.2 Truck-induced Data	36
	3.2.3 Ambient Wind Data	36
	3.3 Summary of Response	38
4	ANALYTICAL PROCEDURE	39
	4.1 Rigorous Analysis	39
	4.1.1 Development of Loading Function	41
	4.1.2 Double Cantilever	43
	4.1.3 Single Cantilever	52
	4.2 Preliminary Program	53
5	ANALYSIS OF RESULTS	56
	5.1 Anchor Bolt Stress Ranges	56
	5.2 Fatigue Analysis	61

Chapter	Page
6 CONCLUSIONS AND RECOMMENDATIONS	68
BIBLIOGRAPHY	70

L I S T O F T A B L E S

Table		Page
2.1	Anemometer Calibration	13
3.1	Ratio of Member Axial Force to Chord 4 Axial Force	26
3.2	Truck-induced Forces	31
4.1	Double Cantilever Experimental vs Analytical Natural Frequencies	43
4.2	Double Cantilever Experimental vs Analytical Base Forces	50
4.3	Single Cantilever Experimental vs Analytical Natural Frequencies	52
4.4	Single Cantilever Predicted Base Forces	52
5.1	Maximum Anchor Bolt Stresses Associated with Table 3.2	62

L I S T O F F I G U R E S

Figure		Page
1.1	Single degree of freedom system	2
1.2	Cantilever signs investigated	5
2.1	Dimensions of double cantilever sign	7
2.2	Strain gage locations on double cantilever	8
2.3	Dimensions of single cantilever sign	10
2.4	Strain gage locations on single cantilever	11
2.5	Forces measured by strain gages	12
2.6	Anemometer and wind vane mount	14
2.7	Recording equipment	16
3.1	Truck-induced strains in double cantilever truss members	19
3.2	Strain traces from a vertical forced vibration test of double cantilever sign	22
3.3	Strain traces from a horizontal forced vibration test of double cantilever signs	23
3.4	Forces acting on base of structure	27
3.5	Wind-induced strains in double cantilever truss members	32
3.6	Strain traces from a vertical forced vibration test of single cantilever sign	34
3.7	Strain traces from a horizontal forced vibration test of single cantilever sign	35
3.8	Truck-induced strains in single cantilever	37
4.1	Modeling of truss-to-support connections	40
4.2	Simulated truck-induced loading	42
4.3	Analytical model of double cantilever sign	44
4.4	Analytical model of single cantilever sign	45
4.5	Analytically derived and normalized chord member forces for double cantilever sign	48

Figure		Page
4.6	Analytically derived and normalized diagonal member forces for double cantilever sign	49
4.7	Normalized force outputs for chord member 4 of double cantilever	51
4.8	Simplified single cantilever analytical models . .	54
5.1	Double cantilever support-to-foundation connection	57
5.2	Forces acting on anchor bolts	59
5.3	Base torque range, T_R , as a function of base shear range, $V_{R,y}$	64
5.4	Histogram of torque range, T_R	66

C H A P T E R 1

INTRODUCTION

1.1 Objectives

A recent fatigue failure of the anchor bolts in a highway sign structure indicated that consideration be given to fatigue in their design, a practice not required in the present AASHTO Specifications. In order to provide a basis for a fatigue design procedure, a determination of the fatigue load must be made.

The fatigue failure which occurred appeared to have been caused by horizontal loads on the structure. Field observations indicated that trucks passing under the sign and wind gusts produce such loads. The appreciable number of stress cycles resulting from these gust loadings can cause the fatigue cracking observed in the anchor bolts.

The objective of this study was to determine the nature and magnitude of these gust loadings on sign structures and the resulting stresses in the members. This was attempted both experimentally and analytically. The variables included in the study were sign structure geometry, vehicle speed, spatial relationship of vehicle and sign, vehicle type, and ambient wind roughness influences on the dynamic behavior of sign structures. The study does not consider the effects of the Von Karman vortex shedding forces on the structure.

1.1.1 Dynamic Response. The response of a structure depends on its mass, damping, stiffness, and the applied loading. These properties are shown in the model of a single degree of freedom (SDOF) system of Fig. 1.1.

The equation of motion [1]* for this system is given as

$$M \ddot{u} + C \dot{u} + K u = P(t)$$

where M = mass of the system

C = damping of the system

K = stiffness of the system

$P(t)$ = applied load

u, \dot{u}, \ddot{u} = displacement, velocity, and acceleration of system

The undamped circular frequency of the system is given by the equation [1]

$$\omega = \sqrt{\frac{K}{M}}$$

If the applied load on a lightly damped system is periodic with a frequency, ω , resonance can occur and result in a large dynamic response. Therefore, damping cannot be overlooked. It is usually expressed as a percentage, known as the damping ratio, given by the equation [1]

$$\xi = \frac{C}{2M\omega} \times 100$$

and having values up to approximately 3 percent for steel structures. Since damping reduces the magnitude of stresses versus time, the determination of ξ is necessary for an analysis. In the case of light damping, about 1 percent, stress amplitudes will decay slowly and the number of cycles will be large. This becomes critical in estimating fatigue life, particularly if the stresses are of significant magnitude.

These concepts can be extended to a multi degree of freedom (MDOF) system, such as a highway sign. The equations of motion [1] become

$$[M] \{\ddot{u}\} + [C] \{\dot{u}\} + [K] \{u\} = \{P(t)\}$$

*Numbers in brackets refer to the Bibliography.

These yield as many natural frequencies and corresponding displacement mode shapes for the structure as the number of degrees of freedom considered in the analysis. To prevent resonance, it is important to know the frequency(ies) of the loading and the natural frequencies of the proposed structure. It must be noted that during a random loading, such as wind gusts, dynamic response can occur even though the load has no regular periodicity, because the structure may respond to a particular component of the load having frequency close to the structure's.

The experimental results (natural frequencies, damping ratios, stress ranges) for the signs instrumented are therefore essential in calibrating the analytical procedure.

1.2 Experimental Program

Two sign structures, a double and single cantilever, shown in Fig. 1.2, were selected for instrumentation. This included strain gages, yielding stresses at particular points of the structure, and anemometers and a wind vane which gave an indication of the wind speed and direction. For each event recorded, the nature of the gust (whether due to a truck or the wind) was noted, as were the type of truck, its approximate height, and its velocity.

1.3 Analytical Program

To investigate the response of a sign structure, an analytical model was used and was subjected to impulses simulating gust loadings. A preliminary computer analysis of the single cantilever was made, using a program written for a consistent mass, 12 DOF system. This was followed by a more sophisticated analysis of both signs using SAP IV, a structural analysis program developed at the University of California [2].

CHAPTER 2

EXPERIMENTAL PROCEDURE

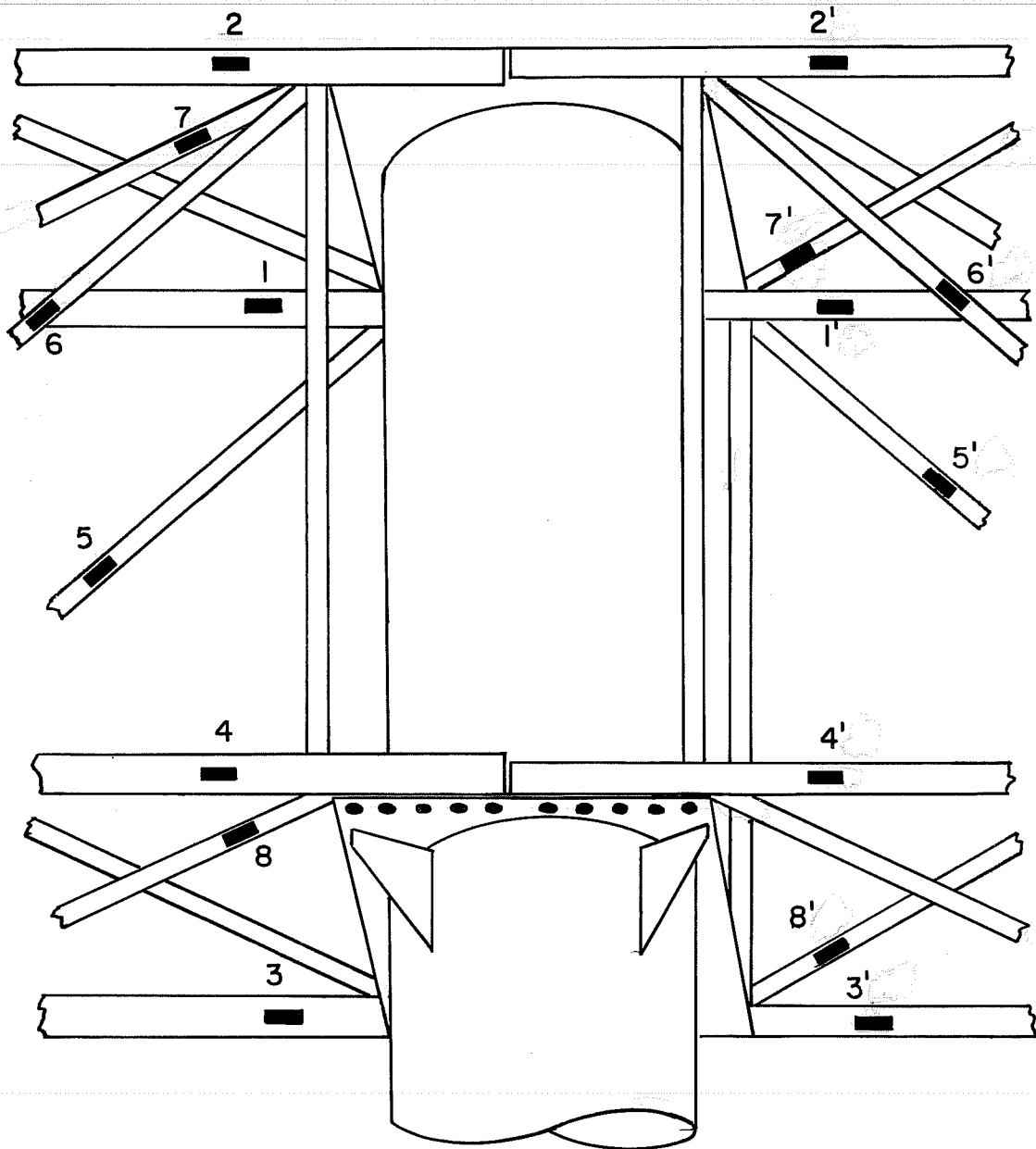
2.1 Sign Selection

The selection of the signs instrumented was governed by

- (a) Accessibility of sign
- (b) Safety from road hazards during the experiment
- (c) Traffic volume
- (d) Type of sign under investigation, i.e., single or double cantilever
- (e) Freedom of wind turbulence due to other structures

The lack of accessibility to signs on Interstate Highway 35 did not allow instrumentation of any signs there. The first sign chosen was the double cantilever (Fig. 1.2a), located at the intersection of Highways 183 and 290 in northeast Austin. The majority of traffic flow at this location is on Highway 183. The centerline of the sign face is 2 ft. from the centerline of the curb lane in Highway 183, as shown in Fig. 2.1.

In addition to the determination of the stresses and the corresponding magnitudes of the loadings in selected truss members on the Highway 183 side of the sign, stresses were also obtained for members on the other side of the support. It was then possible to examine the effect of the second arm (over the exit ramp) and sign face on the dynamic response of the structure and the possible reduction in the resultant base torque due to the aerodynamic resistance of the sign not subjected to truck-induced gusts. The dimensions of this sign are shown in Fig. 2.1 and the location of strain gages is shown in Fig. 2.2.



U.S. 183

U.S. 290

Fig. 2.2 Strain gage locations on double cantilever

The second sign instrumented was the single cantilever (Fig. 1.2b), having a braced tee-mount support and located at the intersection of Highways 290 and 71 in southwest Austin. The traffic flow under the sign was not large and traffic velocity was slow due to a stoplight immediately in front of the sign. The centerline of the sign face is 4.5 ft. from the center of the curb lane, as shown in Fig. 2.3. This sign was chosen because of its similarity to a sign which had experienced fatigue cracking and for the acquisition of ambient wind data. The dimensions of this sign are shown in Fig. 2.3, and the location of strain gages is shown in Fig. 2.4.

2.2 Instrumentation

2.2.1 Strain Gages. The stresses induced in the truss members were measured using strain gages. It was therefore possible to compute horizontal and vertical shears and moments in the truss, and the resulting base torque. These forces are shown schematically in Fig. 2.5.

Polyimide-backed, foil strain gages (BLH N. FAE-50-1256-ES, with a gage length of 0.5 in.) were used. To mount the gages a 2 in. square area of the galvanized coating of the truss members was ground off and sanded smooth at the desired locations. The finished surfaces were cleaned with acetone and then treated with neutralizer to prepare the surfaces for the strain gages. These were then bonded to the surfaces using Eastman 910 adhesive. To facilitate mounting, lead wires had been attached to the gages prior to the field work. The waterproofing consisted of two layers of BLH Barrier B, followed by a BLH Barrier E patch, covering the gage and the lead wire connection. The patch covered an area of about 2 in.².

The leads were then soldered to 40 ft., 3-wire shielded cable. This length was required to ensure access to the recording instruments at the ground level.

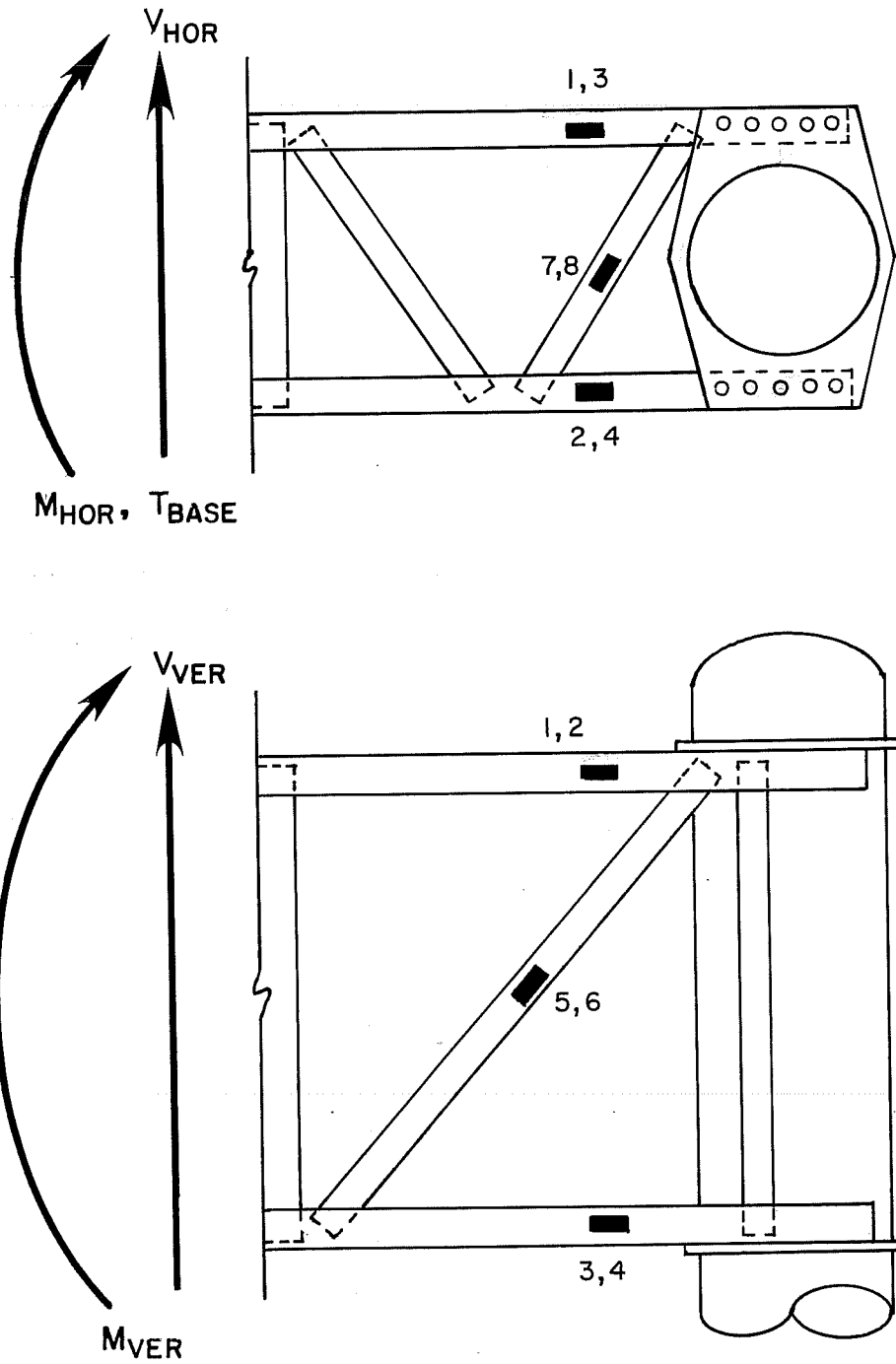


Fig. 2.5 Forces measured by strain gages

2.2.2 Wind-sensing Equipment. For each sign a mount was constructed to attach both a wind vane and an anemometer to the support at the height of the center of the sign face, as shown in Fig. 2.6. It was thus possible to determine the velocity and direction of the ambient wind at the sign face. An attempt at determining the magnitude of the gust by placing an anemometer in front of the sign face was not successful.

Fast response (1.0 - 1.2 mph threshold), 3-cup Gill anemometers were used to measure horizontal wind velocity. There were calibrated in accordance with the manufacturer's suggestions, and produced the voltage outputs shown in Table 2.1

TABLE 2.1 ANEMOMETER CALIBRATION

Output* (Volts)	
Double Cantilever	Single Cantilever
2.36	2.36

*At 1800 rpm corresponding to a 50 mph wind.

Linear interpolation yielded intermediate velocities. To determine the direction of the wind relative to the sign face, a Gill high-sensitivity wind vane was used. This enabled determination of the component of the ambient wind normal to the sign face.

2.2.3 Recording Equipment. A Hewlett-Packard model 7100 B, two-channel, strip chart recorder was initially used for recording wind velocity. Wind direction was monitored visually and noted on the recording chart paper.

A ten-channel, variable gain (1x, 1000x), low-noise amplifier was developed at the Civil Engineering Structures Research Laboratory of The University of Texas Balcones Research Center for this



Fig. 2.6 Anemometer and wind vane mount

project. The high gain of the amplifier was required to allow measurement of very small strains. The signals from the strain gages constituted the input to the amplifier. The amplifier output was connected to a Brush eight-channel, strip chart recorder, model RD1 684-00. The recorder produced a trace of dynamic strains with respect to time.

All the recording equipment was placed in a van which allowed recording during periods of rain. The setup is shown in Fig. 2.7.

2.2.4 Power Supply. A portable 110-volt generator was used to power all the equipment during the experiment.

2.3 Data Accumulation

The measurement of the structure's dimensions (including member thicknesses, etc.) and the placement of strain gages and wind sensors on the single cantilever required two days. For the double cantilever this was done in two stages. First, only the arm over Highway 183 was instrumented. After concluding that the procedure was successful, the other arm was instrumented.

Access from the ground to the truss was accomplished using a 30-ft. long extension ladder. Thus, the strain gage and wind sensor cables could be lowered prior to data acquisition and raised and secured (at the connection of the truss and support) at its conclusion.

Prior to data acquisition, the eight-channel recorder was calibrated in the field to ensure accuracy of the output. Since one channel of the amplifier malfunctioned, it was decided to connect six strain gages and the anemometer to the recorder. The resulting traces facilitated noting the effects of wind gustiness on the response of the structure, with or without trucks passing under the sign.

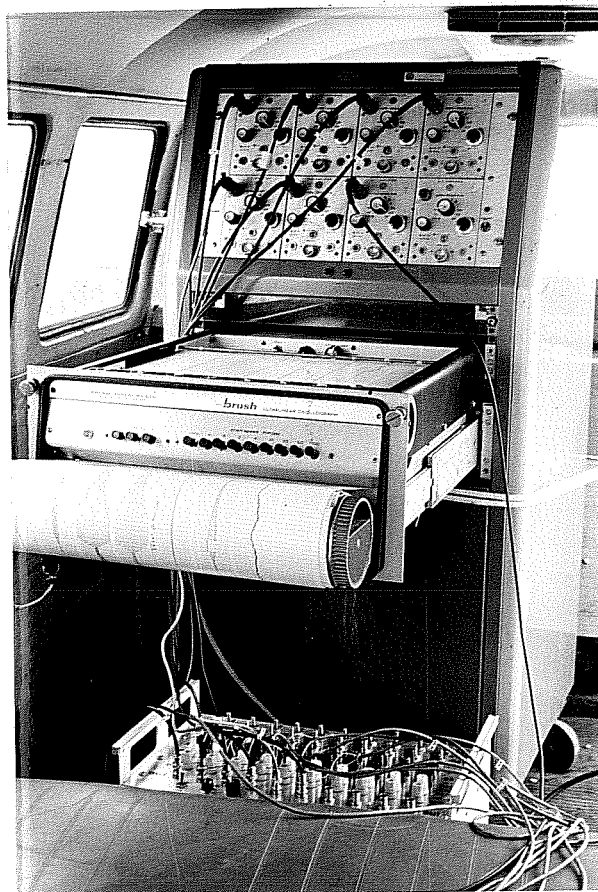


Fig. 2.7 Recording equipment

The strain gages connected to the recorder were chosen based on the required force components (horizontal and vertical shears and moments). It was also possible to connect up to two gages to the two-channel recorder.

The type of data (whether due to ambient wind or to a truck), the wind direction, the recorder's sensitivity setting, and the chart paper's speed were noted on the chart paper.

CHAPTER 3

EXPERIMENTAL RESULTS

3.1 Double Cantilever

A typical dynamic strain output for a single truck passing under the long arm of the sign is shown in Fig. 3.1. The strains shown are for four chord members, one horizontal diagonal, and the anemometer. The location in the sign structure of members and their numbering is as shown in Fig. 2.2.

From traces such as those of Fig. 3.1, it was possible to calculate the stress ranges in the members, the wind velocity, the natural frequency of the structure, and the damping ratio. The traces also provided an indication of whether the motion was predominantly horizontal, vertical, or a combination of these modes.

To calculate the stress range, the number of divisions on the strip chart paper between adjacent positive and negative peaks of a trace were measured. This number provided the range in one cycle of load. The stress range was then computed by the equation

$$S_R = N \times \frac{2.00}{G.F.} \times G \times E$$

where S_R = stress range in ksi

N = number of divisions between peaks

G.F. = gage factor of the strain gage

G = amplifier recorder system gain

E = modulus of elasticity for steel, taken as 29×10^3 ksi

Since the primary interest was in the maximum stress range, most often found in the first three cycles, only that value was

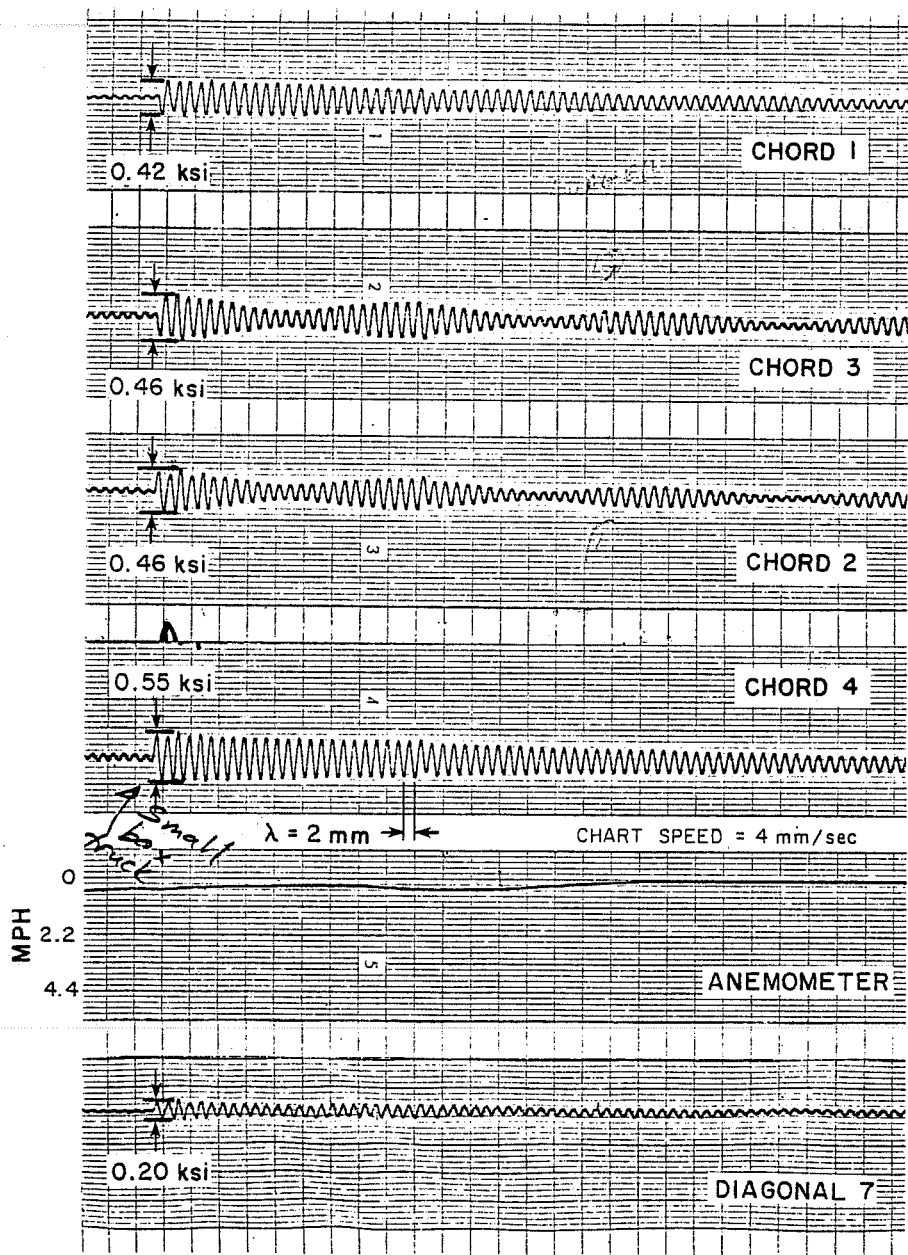


Fig. 3.1 Truck-induced strains in double cantilever truss members

calculated. The maximum stress range for each trace shown in Fig. 3.1 is included in the figure. The 0.55 ksi stress range of chord member 4 is the largest truck-induced stress range recorded in this study. This indicated that the superstructure stresses were low and presented no fatigue problem.

The wind speed was calculated by multiplying the number of divisions of the anemometer trace from its base line times the appropriate recorder gain and anemometer calibration factors. The ambient wind velocity shown in Fig. 3.1 is less than 1 mph.

The natural frequency and its inverse, the natural period, could be calculated by measuring the wavelength of the trace and dividing it by the chart paper speed. For example, the wavelength of the trace for chord number 4 shown in Fig. 3.1 is 2 mm and the chart paper speed was 4 mm/sec; the natural frequency of vibration is, therefore, 2 cycles per second and the natural period 0.5 sec.

The effects of damping on the structure are seen in the progressive decay of the strain amplitudes of the traces shown in Fig. 3.1. This decay can be characterized by the damping ratio ξ . The large number of cycles in the trace indicate that the value of ξ must be small. The procedure for calculating ξ is given in Sec. 3.1.1.

The degree to which the motion, during the structure's response to a load, was in a specific plane or planes was determined by the extent of the response in the chord, the vertical, and/or horizontal diagonal truss members. For example, the trace for the horizontal diagonal member 7 in Fig. 3.1 indicated that the truss had been excited horizontally. This is also shown by the traces of the four chord members. For a horizontal movement of the truss, the stresses in chord members 1 and 3 would be in phase, i.e., their traces would occur on the same side of their baselines simultaneously and opposite in sign to the stresses in chord members 2 and 4 which

would be in phase with each other. For a vertical movement of the truss, the stresses in chord members 1 and 2 would have to be in phase and opposite in sign to the stresses in chord members 3 and 4. Forced vibration tests of the structure, discussed in the following section of this chapter, and various combinations of gages were used to determine the predominant type of motion that was taking place during the response.

Finally, a cyclic increase and decrease in the stress ranges of chord members 2 and 3 is seen in the corresponding traces shown in Fig. 3.1. This response, known as beating, can be attributed to a transfer of energy from one mode to another, or simply a mixing of modes.

3.1.1 Dynamic Characteristics. The beating noted in chord members 2 and 3, which are located diagonally apart, suggested that a transfer from a horizontal to a vertical bending mode of the sign truss was occurring and resulting in biaxial bending in the truss. This biaxial bending would cause the stresses in chord members 1 and 4 to add and stresses in chord members 2 and 3 to subtract, if these two modes have natural frequencies which are numerically close to each other.

To accurately determine the value of the natural frequencies and the damping ratio, the behavior of the structure was examined when subjected to a forced vibration. This was accomplished by standing on the truss as close to the support as possible so as to decrease the effects of the added mass, and rocking the truss either vertically or horizontally. This procedure was repeated several times and produced outputs as shown in Figs. 3.2 and 3.3. It was thus possible to calculate the natural frequencies and damping ratio for the horizontal and vertical deflection modes. The natural frequencies were calculated for four traces of each mode and yielded values ranging from 1.89 to 1.90 cycles per second

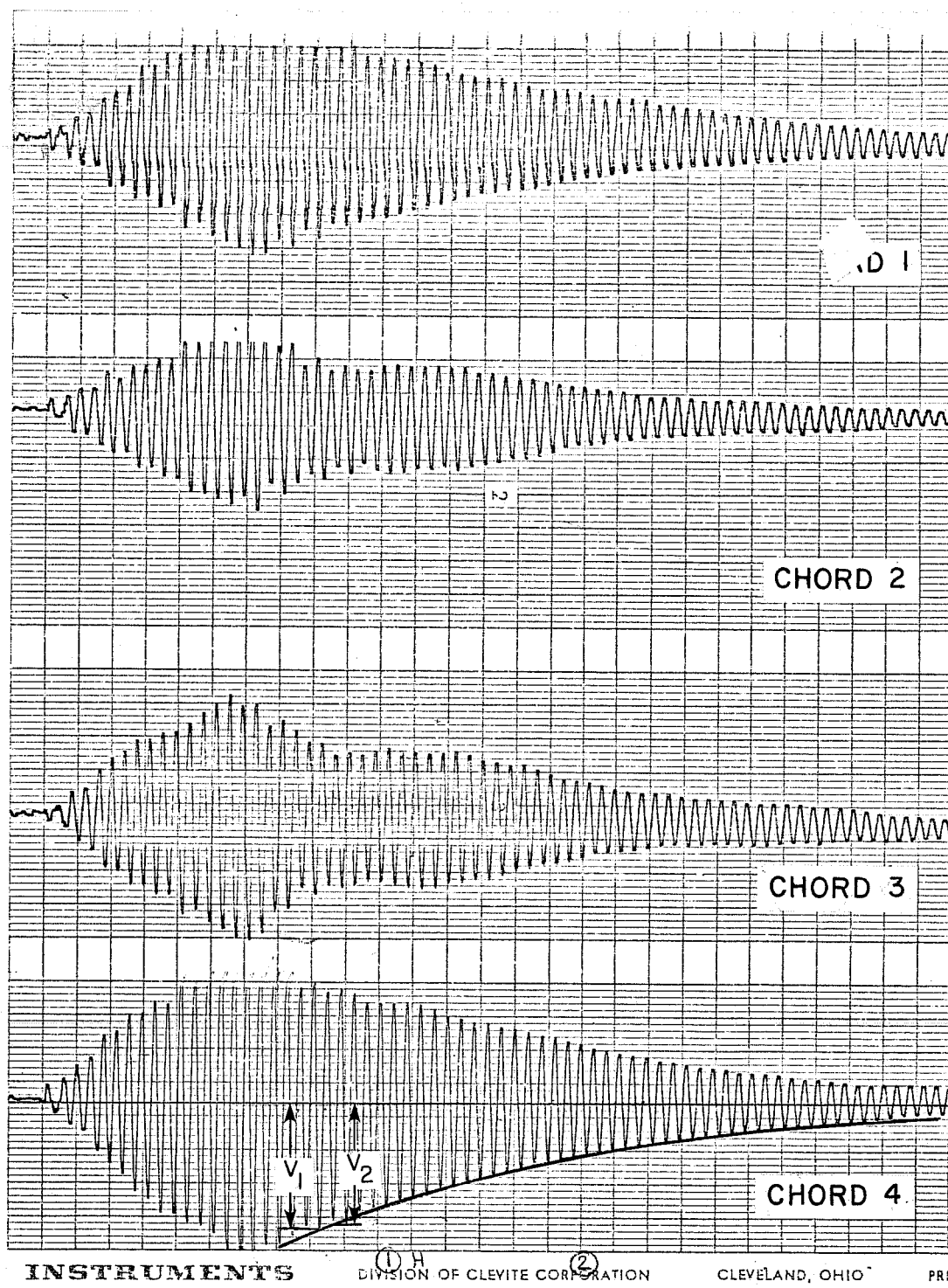


Fig. 3.3 Strain traces from a horizontal forced vibration test of double cantilever signs

for the vertical mode, and 2.0 to 2.04 cycles per second for the horizontal. The average values for the first mode natural frequency and period are 1.90 cycles per second and 0.53 seconds, respectively. For the second mode these values are 2.01 cycles per second and 0.50 seconds, respectively.

The closeness of these values strengthened the belief that the beating noted in the outputs was caused by a mixing of the first and second modes.

The damping ratio, ξ , was estimated using the logarithmic decrement given by the equation [1]

$$\xi = \frac{\ln \frac{V_1}{V_2}}{2\pi} \times 100$$

where ξ = damping ratio in percent of critical

V_1 = initial strain amplitude

V_2 = strain amplitude immediately following V_1

The amplitudes were estimated by drawing a curve best fitting the peaks in a trace and measuring the number of chart paper divisions from the peaks to the baseline of the trace, as shown in Fig. 3.3.

The damping ratio was calculated for four pairs of points in two forced vibration tests of the first mode. The calculated values ranged from 0.40 to 0.60 percent of critical, with a mean of 0.49 percent of critical and a standard deviation of 0.08 percent. Six pairs of points from three tests were used to calculate ξ for the second mode. The calculated values ranged from 0.61 to 0.80 percent of critical with a mean value of 0.69 percent of critical and a standard deviation of 0.08 percent. These values of ξ are much less than the 3 percent generally used in steel structures. The low value of damping accounts for the large number of stress cycles following passage of the truck shown in Fig. 3.1.

The vertical forced vibration test, shown in Fig. 3.2, indicated that chord member 4 was not stressed as much as the other chords. An explanation of this could be that although the truss moves primarily vertically, it also rotates about chord member 4, thereby stressing the other chords more. Verification of this was not possible, since no displacement or acceleration records were made to determine the precise displacement made. This behavior may also explain why chord members 1 and 4 did not exhibit beating.

3.1.2 Truck-induced Data. An example of truck-induced dynamic strain records was shown in Fig. 3.1. The limited numbers of recording channels did not allow simultaneous data acquisition of all sixteen gages shown in Fig. 2.2. Various combinations of gages were used to obtain an understanding of the response of all members instrumented.

The following procedure was used to estimate the maximum stress range and corresponding axial force ranges in the members for which strains were not recorded for a particular event. Chord member 4 consistently exhibited the highest force range of all members in any recording event of truck-induced response. Ratios of the maximum force ranges for each of the other member strains recorded to that for chord member 4 were calculated for several events and an average value was taken. An example of this are the force ratios obtained from the traces shown in Fig. 3.1. The ratios of maximum force ranges of chord members 1, 2, 3, and diagonal member 7 to the maximum force range of chord member 4 are 0.78, 0.83, 0.84, and 0.15, respectively. The maximum force range in members whose strain gages were not connected to the recorder during an event were estimated using these average ratios. In the case where the response of chord member 4 was not recorded but that of another chord member had been, an approximate value for the force range in chord member 4 would be estimated using the inverse of the ratio previously calculated for the other chord member. It is clear that

the resulting force ranges are approximate and are more accurate in the case where the actual force ranges in chord member 4 are known. Table 3.1 gives the average value for the ratio of maximum member force ranges to that of chord member 4 for twenty-two events recorded.

TABLE 3.1 RATIO OF MEMBER AXIAL FORCE TO CHORD 4 AXIAL FORCE

MEMBER	1	2	3	4	1'	2'	3'	4'	5	6	7	8	5'	6'	7'	8'
RATIO	-0.74	0.81	-0.83	1.0	-0.23	0.21	0.31	-0.33	-0.09	-0.11	0.17	0.23	0.04	0.10	0.06	0.10

NOTE: Values are based on experimental truck-induced data.

The values given in Table 3.1 indicate that the bottom chord members of the truss on either side of the support, members 3, 4, 3', and 4', are stressed higher than the top chord members. This implies that the bottom chord members are subjected to a higher load than the top chord members, suggesting that the loading on the sign could be modeled as a pressure distribution decreasing with increasing height. This information was used to develop the loading used in the analytical study. In addition, a significant difference in axial force exists between the corresponding chord members on either side of the support, i.e., chord member 3 is subjected to a force approximately 2.5 times that in chord member 3'.

The force in each of the four diagonal truss members, two in each side of the support, as shown in Fig. 2.2, which had not been instrumented, was assumed to be equal and opposite to that in the gaged member. The analytical results verified this assumption.

The torque, biaxial shears and moments at the base of the sign, shown schematically in Fig. 3.4, were calculated from the member forces in the sign truss. In the equations given below, summation of forces in members refers to members on both sides of the support unless otherwise stated.

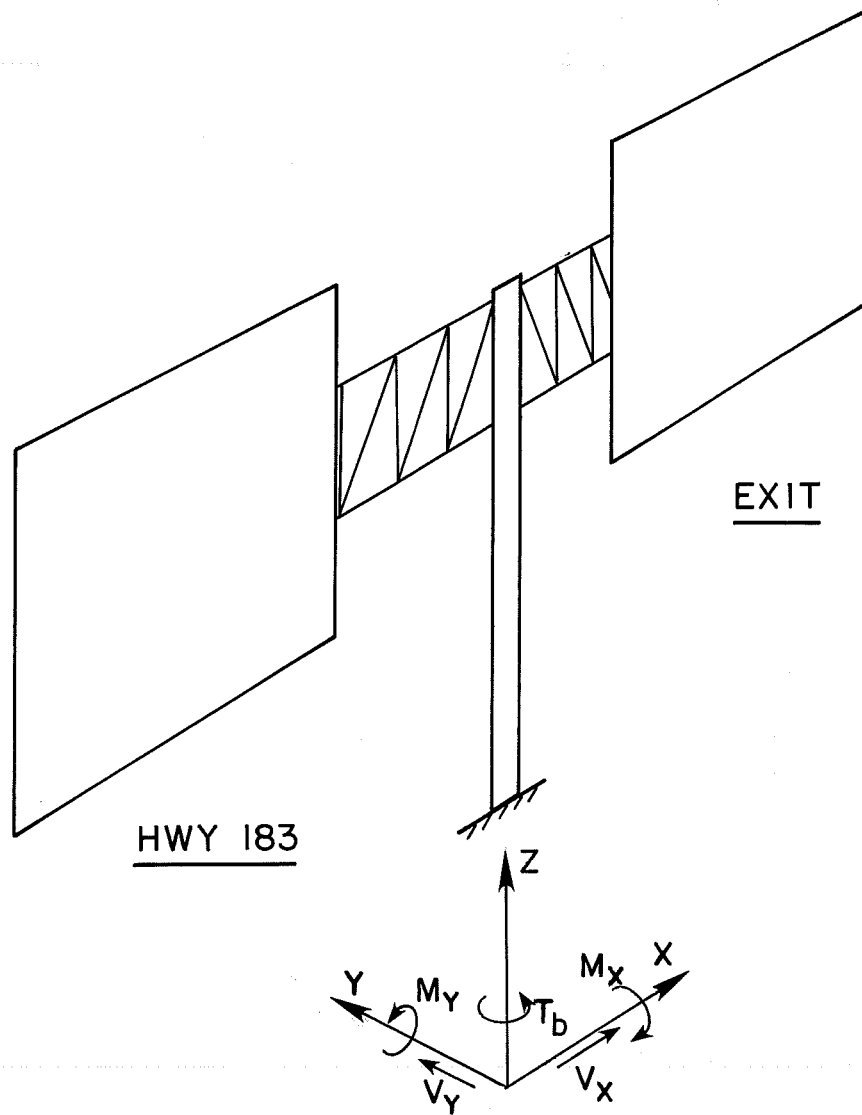


Fig. 3.4 Forces acting on base of structure

The maximum base torque results when the chord member forces are maximum. The torque is given by the equation

$$T_b = [(\text{summation of the forces in chords 1, 3, 1', and 3'}) \\ + (\text{summation of the forces in chords 2, 4, 2', and 4'}) \\ + (\text{summation of the forces in horizontal diagonal members}) \\ \times \cos \alpha \\ + (\text{summation of the forces in vertical diagonal members}) \\ \times \cos \beta] \times e$$

where T_b = base torque

α = angle between chord and horizontal diagonal members,
27.3°

β = angle between chord and vertical diagonal members,
36.9°

e = distance from centerline of support to centerline of chord, 16.5 in.

The base shear, V_y , in the direction of traffic, caused by the horizontal gust loadings on the sign face due to trucks, can be estimated by the equation

$$V_y = [\text{summation of forces in horizontal diagonal members}] \\ \cdot \sin \alpha$$

where V_y = base shear in the direction of traffic

$\alpha = 27.3^\circ$

The base shear, V_x , in the direction parallel to the length of the truss was calculated from the equation

$$V_x = [\text{summation of chord member forces} + (\text{summation of} \\ \text{vertical diagonal member forces}) \times \sin \beta + (\text{summation} \\ \text{of horizontal diagonal member forces}) \times \cos \alpha]$$

where V_x = base shear in the direction parallel to the length of the truss

$\beta = 36.9^\circ$

$\alpha = 27.3^\circ$

The base overturning moment, M_x , in the direction of traffic is given by the equation

$$M_x = [(\text{summation of top chord horizontal diagonal members}) \times l_1 + (\text{summation of bottom chord horizontal diagonal members}) \times l_2] \times \sin \alpha$$

where M_x = base overturning moment in the direction of traffic

l_1 = moment arm from base plate to top chords, 300 in.

l_2 = moment arm from base plate to bottom chords, 252 in.

$\alpha = 27.3^\circ$

Finally, the base overturning moment, M_y , in the direction parallel to the length of the truss is given by the equation

$$M_y = [(\text{summation of top chord member forces}) + (\text{summation of vertical diagonal member forces}) \times \cos \beta] \times l_1 + (\text{summation of bottom chord members forces}) \times l_2$$

where M_y = base overturning moment in the direction parallel to the length of the truss

$\beta = 26.9^\circ$

$l_1 = 300$ in.

$l_2 = 252$ in.

The summation of the x-direction, horizontal diagonal member forces is zero and is not included.

Based on the equations above, the maximum base force ranges associated with the event shown in Fig. 3.1 were calculated as:

$$T_{\max} = 34.72 \text{ kip-in.}$$

$$V_{y, \max} = 0.094 \text{ kips}$$

$$V_{x, \max} = 0.001 \text{ kips}$$

$$M_{y, \max} = 4.98 \text{ kip-in.}$$

$$M_{x, \max} = 25.43 \text{ kip-in.}$$

These values indicate that for this event, the predominant base forces were the torque, T_b , the overturning moment, M_x , and the shear V_y .

The maximum member and resulting base forces for other events which produced significant forces are given in Table 3.2. The values in this table indicate that the base shear, V_x , in the direction parallel to the length of the truss is considerably smaller than V_y . The values for V_x and M_y are particularly sensitive to small changes in member force values, as the results show for events 2 and 3. It is also evident that box-type trucks produced the maximum measured response. The trucks were either the larger 3-axle trucks, approximately 45 ft. long and 13.5 ft. high, or the smaller 2-axle trucks, approximately 25 ft. long and 11 ft. high. It is interesting to note that the maximum measured response, that shown in Fig. 3.1, was produced by a smaller truck. In addition to box trucks, the structure responded to tank and gravel trucks and buses, although the magnitude of response was much less. Although the speed of a passing truck was not measured, it was estimated that the maximum speed was about 50 mph.

During periods of high wind gusts in a direction parallel to traffic, the response of the structure to truck-induced gusts was negligible. This is attributed to the reduced relative velocity of the truck gust to the sign.

3.1.3 Ambient Wind Data. Wind-induced strains, an example of which is shown in Fig. 3.5, can be significant. The output shown was recorded during a rainstorm and gave a maximum stress range of 0.68 ksi in chord member 4 during the event labeled 7A at a gust wind speed of 12.3 mph. Similar traces indicated that only gusty winds, such as during a storm, produce significant stress ranges and number of cycles. In general, for steady winds, the response was negligible.

TABLE 3.2 TRUCK-INDUCED FORCES

Event	No. of Axles	Maximum Truss Member Axial Force (lbs)																Torque (k-in.)			V _y (k)		V _x (k)		M _y (k-in.)		M _x (k-in.)	
		1	2	3	4	1'	2'	3'	4'	5	6	5'	6'	7	8	7'	8'	(k-in.)	(k)	(k)	(k)	(k)	(k)	(k-in.)	(k-in.)			
1	2	-357	388	-389	466	-107*	98*	144*	-154*	-42*	-51*	19*	47*	70	107*	28*	47*	34.72	0.094	0.001	25.43	-4.98						
2	3	-262	336	-320	388	-89*	81*	120*	-128*	-35*	-43*	16*	39*	60	89*	23*	39*	28.52	0.080	0.049	21.74	11.84						
3	2	-262	285	-275	388	-89*	81*	120*	-128*	-35*	-43*	16*	39*	60	89*	23*	39*	26.93	0.080	0.044	21.74	7.88						
4	3	-244	310	-298	362	-83*	76*	112*	-119*	-33*	-40*	14*	36*	60	83*	22*	36*	26.64	0.078	0.045	21.32	10.28						
5	3	-238	259	-275	362	-83*	76*	112*	-119*	-33*	-40*	14*	36*	50	83*	22*	36*	25.04	0.069	0.023	18.57	2.58						
6	2	-234	228	-249*	300*	-57	55	110	-118	-27*	-33*	12*	30*	51*	69*	18*	30*	23.13	0.066	-0.026	18.10	-10.80						
7	3	-230	244	-277	300	-69*	63*	93*	-99*	-27*	-33*	12*	30*	52	75	18*	30*	23.07	0.072	-0.032	19.76	-11.16						
8	2	-201	224	-249	248	-57*	52*	77*	-82*	-22*	-27*	10*	25*	52	70	15*	25*	20.47	0.075	-0.035	20.58	-10.74						
9	2	-167	207	-229	258	-59*	54*	80*	-85*	-23*	-28*	10*	26*	50	60*	15*	26*	19.16	0.063	0.009	17.49	1.20						

*Values shown are extrapolated from available experimental data and the ratios of Table 3.1.

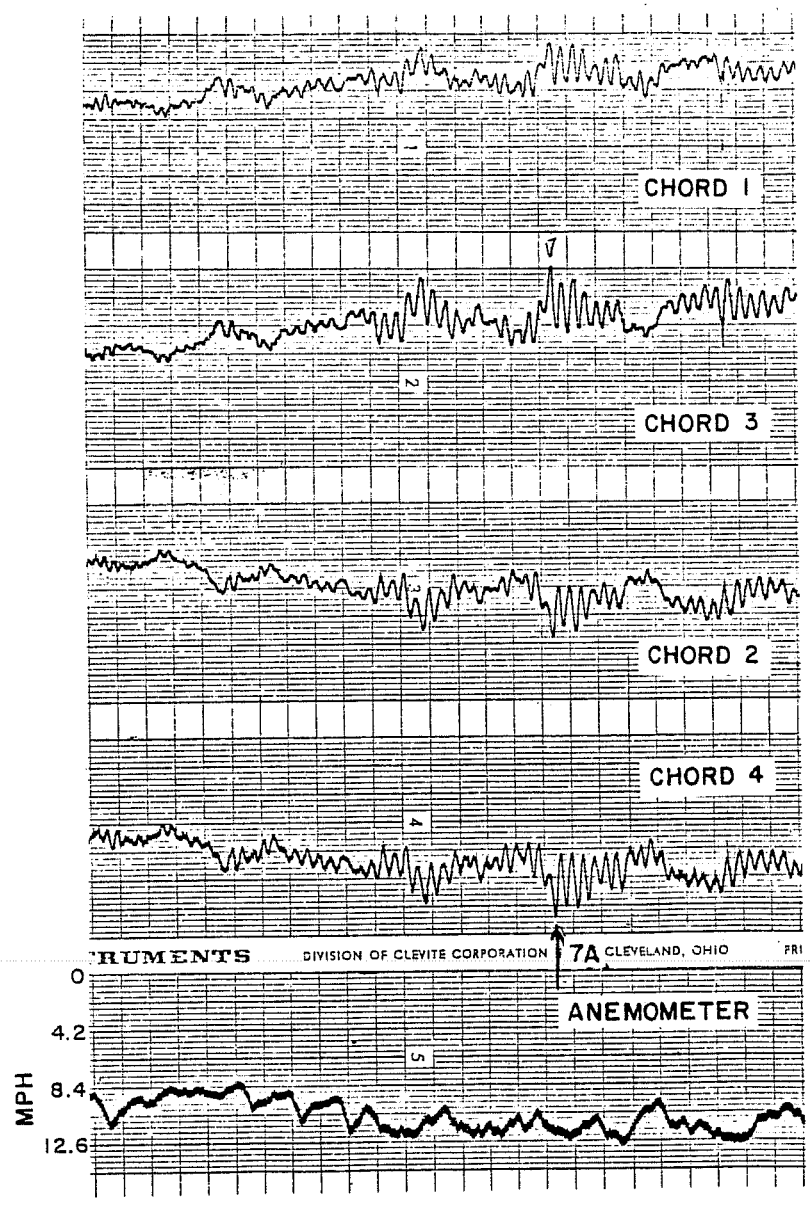


Fig. 3.5 Wind-induced strains in double cantilever truss members

3.2 Single Cantilever

3.2.1 Dynamic Characteristics. Forced vibration of the sign in the vertical and horizontal modes yielded outputs shown in Figs. 3.6 and 3.7, respectively. No beating was indicated in the data. The natural frequencies were calculated for two traces in the first or vertical mode yielding values of 1.55 and 1.56 cycles per second, and for three traces in the second or horizontal mode with values of 1.91 to 1.92 cycles per second. The average values of the first mode natural frequency and period are 1.56 cycles per second and 0.64 seconds, respectively. For the second mode, these values are 1.91 cycles per second and 0.64 seconds, respectively. The absence of beating in the strain traces for this sign is attributed to the large difference between the first and second mode natural frequency values.

The damping ratio was calculated for four sets of points in two traces of the first mode and yielded values ranging from 0.62 to 0.82 percent of critical, with a mean of 0.73 percent of critical and a standard deviation of 0.08 percent. For the second mode, eight pairs of points in five traces were used to calculate ξ and yielded values ranging from 0.64 to 1.11 percent of critical, with a mean value of 0.77 percent of critical and a standard deviation of 0.19 percent. The mean values of ξ are, as was for the double cantilever, much less than the 3 percent generally taken for steel structures. Thus, large numbers of load cycles occur in the structure after application of a load.

It should be noted that in the horizontal mode outputs, the stress ranges in the lower chord members 3 and 4, refer to Fig. 2.4, were approximately four times the magnitude of the stress ranges in the upper chord members 1 and 2. Two possible explanations of this behavior were considered. The first possible explanation was that slip was occurring at the connection of the top chord and the



Fig. 3.6 Strain traces from a vertical forced vibration test of single cantilever sign

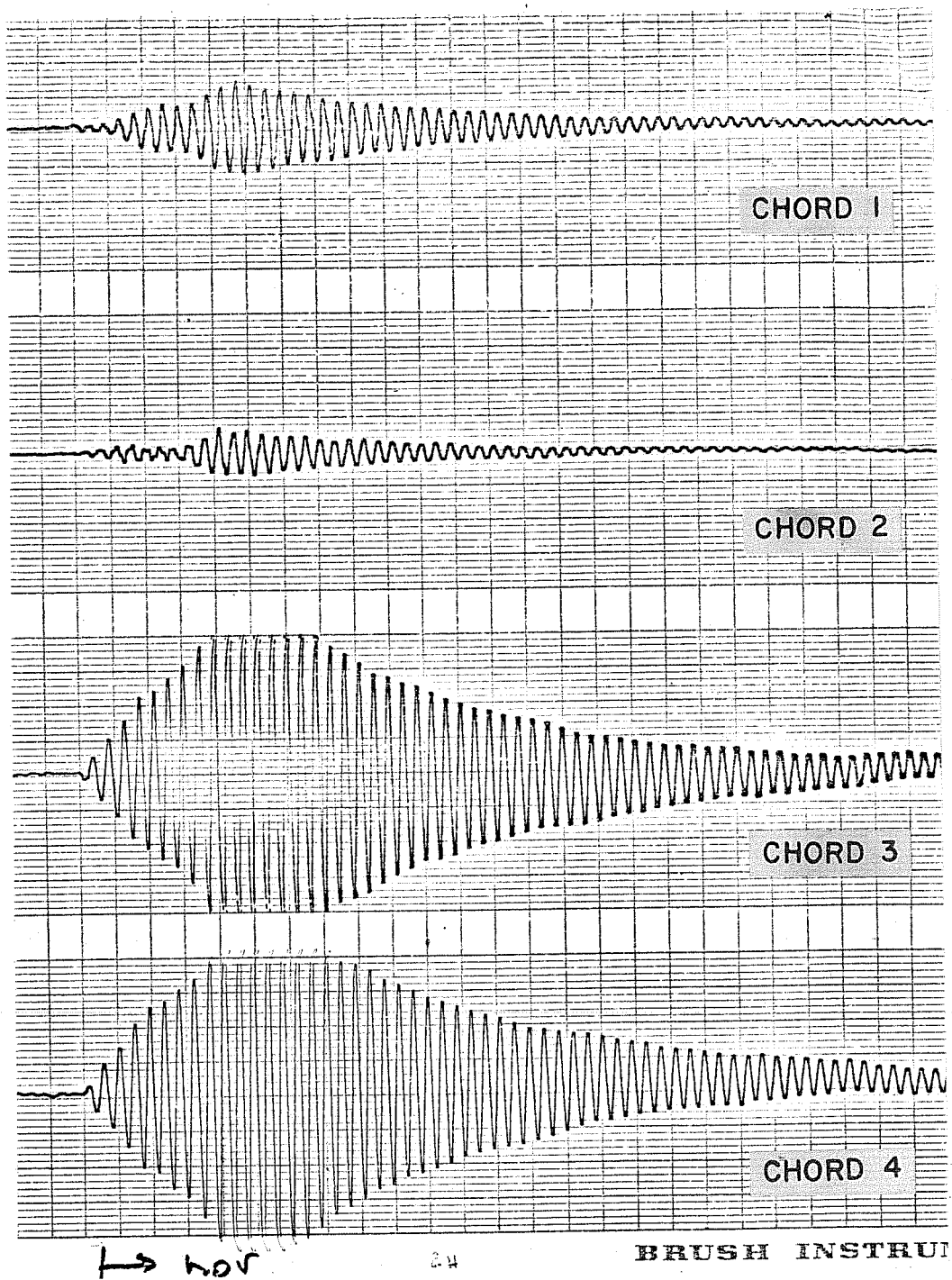


Fig. 3.7 Strain traces from a horizontal forced vibration test of single cantilever sign

support. This connection involves the bolting of the top chord members into a gusset plate which is welded to a sleeve fitting around the vertical pipe support. Two through bolts are used to connect the sleeve and the support. Slip can occur in this two bolt joint due to the oversize holes, as the truss deflects horizontally. This slip would continue until the bolts are in bearing. The lower panel, on the other hand, is bolted to a gusset plate welded to the support. Consequently, no slip occurs between the gusset plate and the support.

The second possibility for the higher stress ranges in the lower chord members is that the truss exhibits shear lag between the top and bottom chords and behaves like a deep beam. The truss relies on the diagonal cross bracing to transmit horizontal shear from loads applied on the lower chord members to the top chord members. This truss is very deep, 5 ft.-4 in., and the inertia force due to the mass of the sign face, the walkway, and lights is larger on the lower chords.

The vertical forced vibration traces, as shown in Fig. 3.6, indicated that chord member 4 was stressed substantially less than the other chord members, similar to the double cantilever. Again, it is believed that the truss, in spite of its vertical motion, also rotates about chord member 4.

3.2.2 Truck-induced Data. Most of the truck-induced response was insignificant, as shown in Fig. 3.8, due to the stop-light ahead of the sign which reduced the speed of the trucks. However, it can be seen that the lower chord members are stressed, whereas the top chord members are not. This result is similar to that of the horizontal forced vibration tests.

3.2.3 Ambient Wind Data. Smooth wind speeds up to 15 mph perpendicular to the sign face produced extremely low chord member

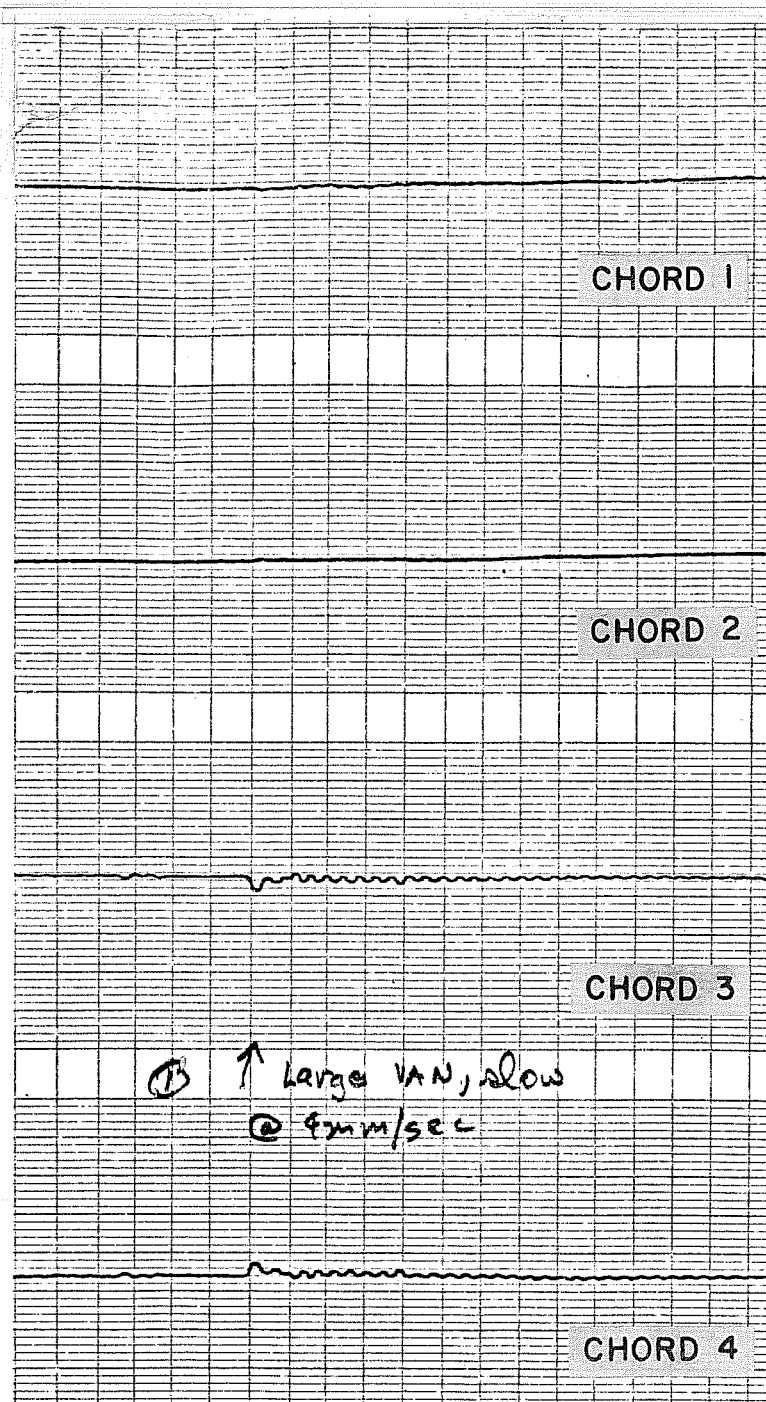


Fig. 3.8 Truck-induced strains in single cantilever

stresses. No significant wind gusts were recorded during the periods data were recorded.

3.3 Summary of Response

Based on the forced vibration test results for both the double and single cantilevers, the first and second mode natural frequencies and periods, and damping ratios were found. The first mode of both signs corresponded to a vertical movement of the sign face with the truss rocking about the vertical support. The second mode for both signs was a horizontal movement of the sign with the truss rotating about the support. The presence of beating in the strain traces for the double cantilever was attributed to the closeness of the first and second mode natural frequencies. No beating occurred in the single cantilever sign.

For both structures, the values of the damping ratios for the first and second modes were very low and accounted for the large number of cycles produced following a truck passage.

In the double cantilever, the overall stress and force analysis of chord and diagonal members showed that chord member 4 was consistently the most highly stressed. For both signs, the lower chords were stressed higher than the top chords, indicating that the load on the sign face decreased with increasing height. This difference in chord stresses was more pronounced in the single cantilever and was attributed to a shear lag between the top and bottom chord members due to the larger truss depth.

C H A P T E R 4

ANALYTICAL PROCEDURE

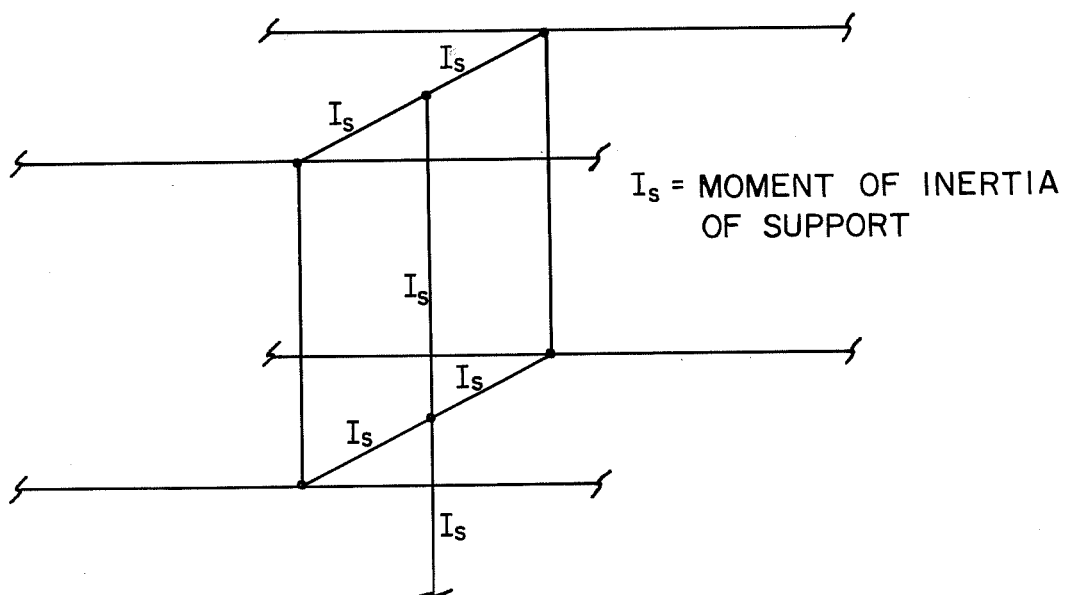
4.1 Rigorous Analysis

A rigorous analysis was made using SAP IV computer program [2]. This program is capable of generating the mass and stiffness matrices of a three-dimensional structure and performing a dynamic analysis of the system. The actual member properties (sizes, mass, modulus of elasticity) were used in the analytical model for each of the two signs instrumented.

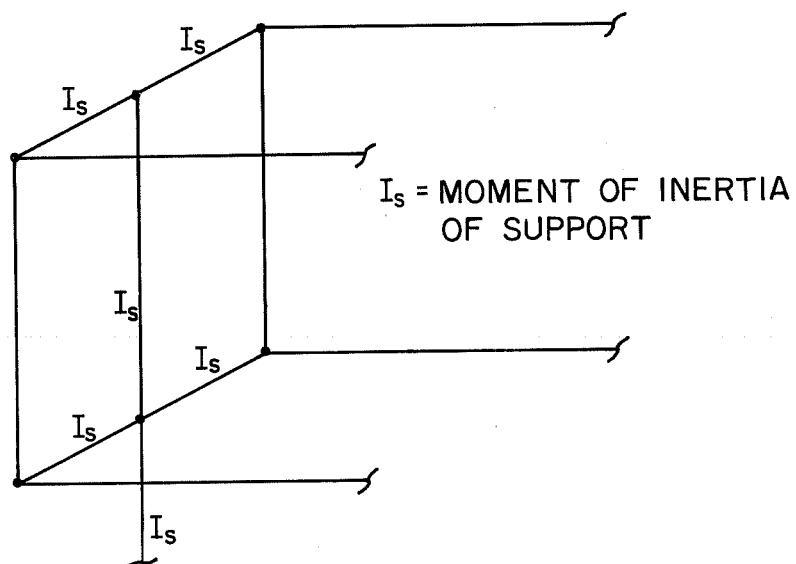
The experimental test data provided the values of the damping ratios for each sign and aided in developing the loading function.

The following approximations were used in the modeling of both signs:

- (a) The sign face, walkway, and lights were input as lumped masses at the models' nodal points on the side facing the direction of traffic.
- (b) The truss to support connections were modeled as shown in Fig. 4.1, with the members connecting the chords to the support having a stiffness equal to that of the pipe support of the sign under investigation to provide the rigidity achieved by the actual connections.
- (c) The support and chord members, since the latter were continuous, were input as beam elements; the remaining members were treated as simply supported truss elements.
- (d) Full base fixity was assumed.



(a) DOUBLE CANTILEVER



(b) SINGLE CANTILEVER

Fig. 4.1 Modeling of truss-to-support connections

4.1.1 Development of Loading Function. A loading function was developed to simulate the gust produced by box-type trucks passing under the sign. The same loading was used in both the double and single cantilever sign analysis.

The experimental results indicated that the truss was excited both horizontally and vertically when a truck passed under the sign. The horizontal load on the bottom chord was thought to be larger than for the top chord. Kyropoulos [3] has shown that box trucks produce both a horizontal and vertical pressure disturbance at the end of the cab. The magnitude of the vertical pressure is approximately equal to the horizontal pressure. Therefore, the lights, which offer resistance to a vertical gust (whereas the mesh of the walkway does not) would be subjected to a uniform vertical pressure distribution. The horizontal pressure distribution on the sign face was assumed to be triangular with a maximum pressure at the bottom of the sign face and zero at the top of the sign face. This distribution was found to give the closest agreement with the experimental results, since a uniform pressure distribution did not give the observed unequal forces between the top and bottom chords. The pressure distribution on the sign face and lights is shown in Fig. 4.2(a).

The shape of the impulse loading function used to simulate the gust caused by a truck is shown in Fig. 4.2(b). The rise time, time to maximum load, and duration of the impulse were calculated using a 30 ft. truck traveling at 50 mph. The duration of the load was calculated as

$$t = \frac{30 \text{ ft.}}{50 \text{ mph}} = \frac{30 \text{ ft.}}{80 \text{ ft./sec}} = 0.375 \text{ sec}$$

A rise time of 0.125 sec was selected, since the maximum wind pressure from a truck occurs behind the cab at the beginning of the box trailer. The rise time corresponds to the time for the first 10 ft. of the truck to pass under the sign. The value of the peak pressure,

p_{\max} , shown in Fig. 4.2(b), was found by matching the analytical member stresses with the member stresses calculated for the data shown in Fig. 3.1. The resulting maximum pressure at the bottom of the sign was equivalent to that produced by a wind velocity of 19.2 mph using the standard equation for wind pressure:

$$p = 0.00256 V^2 C_D$$

where p = pressure in psf

V = wind velocity in mph

C_D = drag coefficient, taken as 1.3

The value for p_{\max} is 1.23 psf.

Since the maximum truck-induced excitation resulted from trucks passing under the sign in the curb lane, the loads on the models for the two signs, shown in Figs. 4.3 and 4.4, were applied only at the numbered nodes. These nodes correspond to the nodes to which the sign face was attached. The proportions of the loads shown depend on the tributary sign area for each node and the pressure distribution on the sign face and walkway. The total load on each node is the coefficient shown in the table in each figure times the pressure.

4.1.2 Double Cantilever. The analytical model of this sign is shown in Fig. 4.3. Good agreement between the experimental and analytical natural frequencies was found, as shown in Table 4.1.

TABLE 4.1 DOUBLE CANTILEVER EXPERIMENTAL VS ANALYTICAL NATURAL FREQUENCIES

Mode	Experimental Frequency (cps)	Analytical Frequency (cps)	% Error
First	1.90	2.00	5
Second	2.01	2.10	4

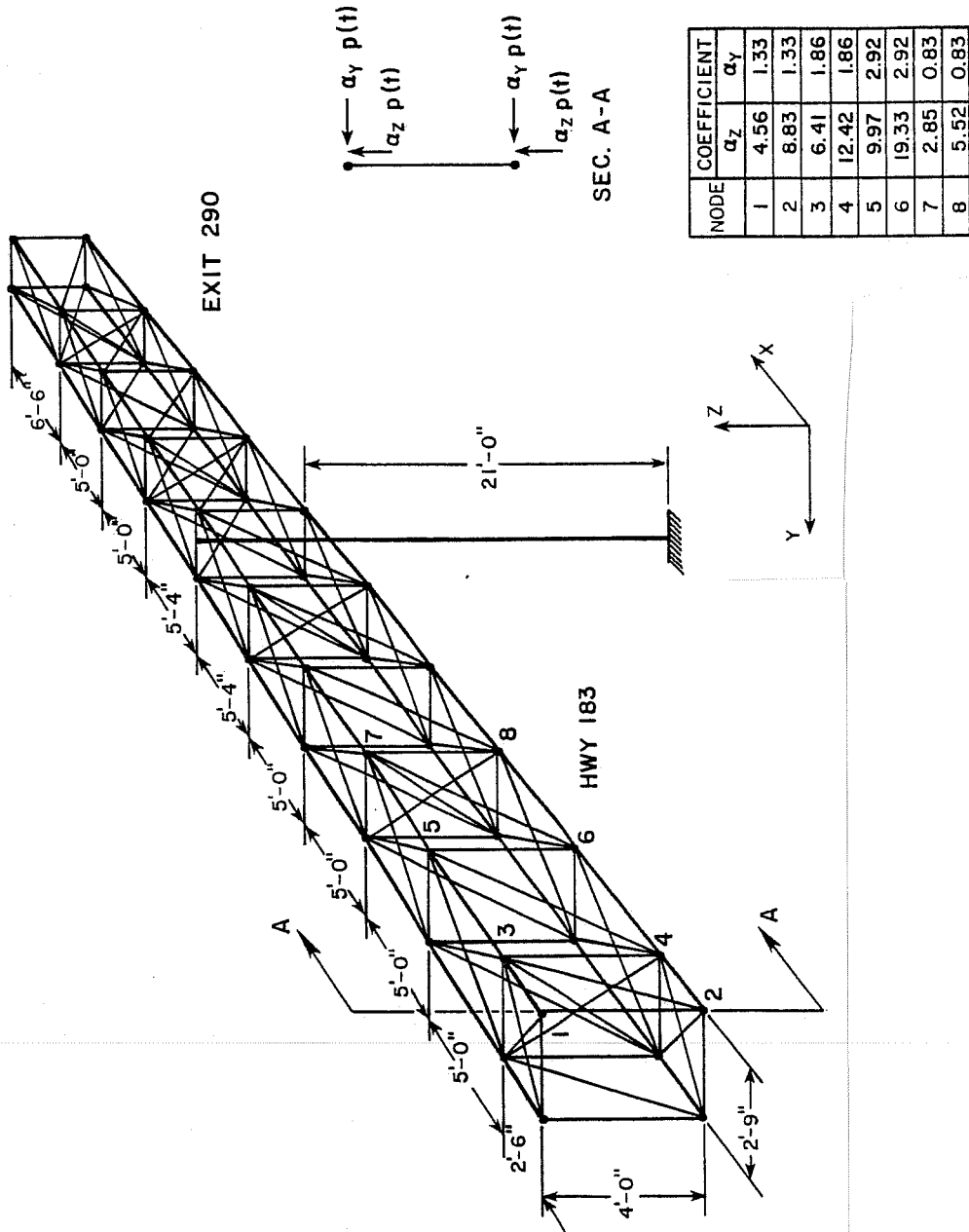


Fig. 4.3 Analytical model of double cantilever sign

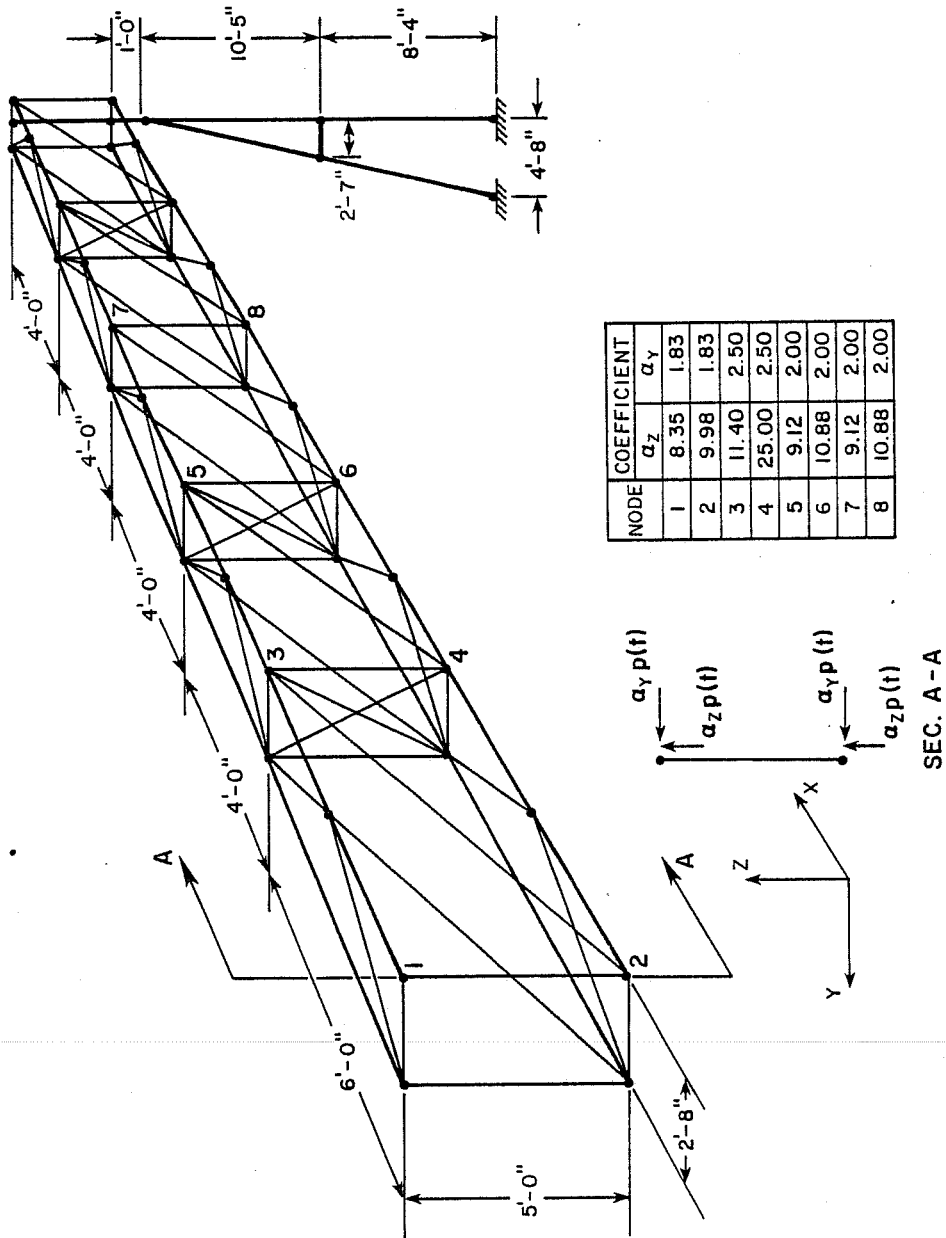


Fig. 4.4 Analytical model of single cantilever sign

The corresponding eigenvectors indicated that the first mode was primarily a vertical rocking of the sign about the vertical pipe support, while the second mode was a horizontal twisting about this support.

The program calculated stress histories at intervals of 0.01 sec for all members for which experimental data existed and for the two diagonals on either side of the support, shown in Fig. 2.2, which were not instrumented. The beating induced was negligible and did not approach the magnitude found in the actual sign.

For a p_{\max} resulting from a 19.2 mph wind speed, good agreement was found in the maxima of axial forces between the analytical and experimental results for the chord members 1, 2, 3, and 4 on the traffic side of the truss shown in Fig. 3.1. However, for the chord members on the arm of the sign over the exit ramp, the analytical solution indicated that the maximum force did not occur at the same time as those in the arm over traffic. The experimental results did not show this difference in the time of occurrence of maximum force. The reason for the difference between the analytical and experimental behavior of the unloaded arm of the truss is not known and will be examined in future work.

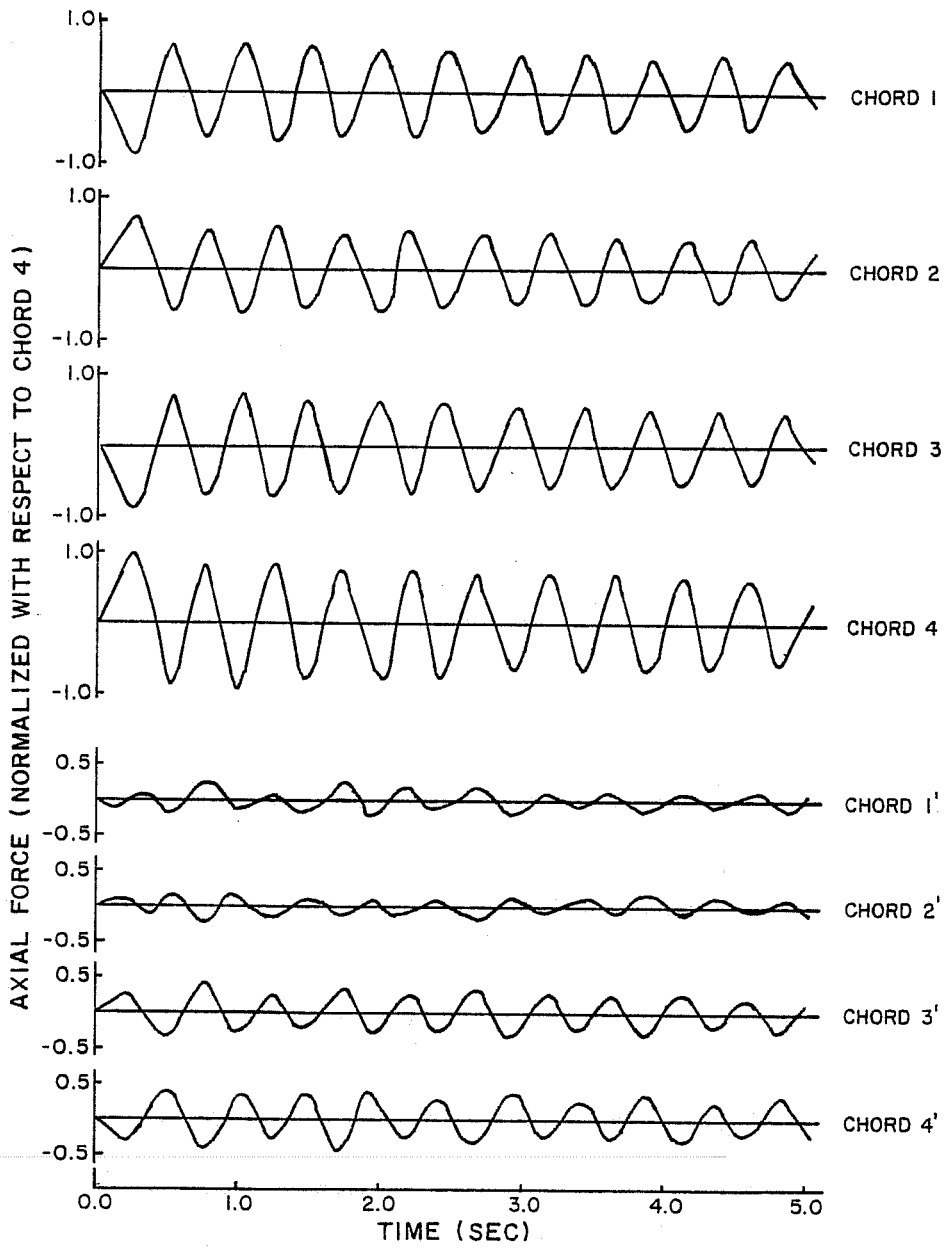
The experimental and analytical results were also compared to determine the significance of the aerodynamic resistance of the sign face on the unloaded arm of the truss. The analytical solution did not consider any aerodynamic forces on the sign face. The chord member forces from the analytical results were larger than those of the experimental. The opposite was expected, since the aerodynamic and inertia forces should be in the same direction. Consequently, the aerodynamic forces on the sign as it moves through the air do not appear to be a simple positive overpressure on the forward face of the sign. Therefore, no conclusions can be drawn on any

aerodynamic resistance of the sign face on the unloaded arm of the truss.

The use of beam elements in the modeling of the chord members accounted for the continuity of these members. It was also necessary to prevent local dynamic instability at locations where members framed into the chord in only one plane, for example between nodes 1 and 3 of the single cantilever shown in Fig. 4.4. The magnitude of end moments and shears resulting from considering the chords as beam elements was negligible. Each chord behaved effectively as a simply supported beam between the nodes. This configuration gave predominantly truss-type behavior.

The analytically derived axial chord and diagonal member forces, normalized with respect to the maximum force in chord 4, versus time are shown in Figs. 4.5 and 4.6. The ratios of maximum axial force to that of chord 4 for the chord members on the loaded arm of the truss and for diagonal member 7 are very close to the values obtained from the traces shown in Fig. 3.1. For chords 1, 2, 3, and diagonal member 7, the analytically derived ratios are 0.83, 0.80, 0.87, and 0.13, respectively, as compared to values of 0.78, 0.83, 0.84, and 0.15 found experimentally. It can be seen in Fig. 4.5 that the maximum forces in the chord members of the unloaded arm of the truss did not occur simultaneously with those of the loaded arm. The maxima of normalized force for these four members vary from approximately 0.21 to 0.48, as compared with 0.21 to 0.33 found experimentally and given in Table 3.1. The analytical solution underestimated the values of normalized force for diagonal members 5, 6, 5', and 6', whereas gave better agreement for diagonal members 7', 8, and 8'.

The predicted behavior of chord member 4 and that obtained from the experimental trace shown in Fig. 3.1 are compared in



NOTE: POSITIVE VALUES FOR
AXIAL FORCE DENOTE
TENSION

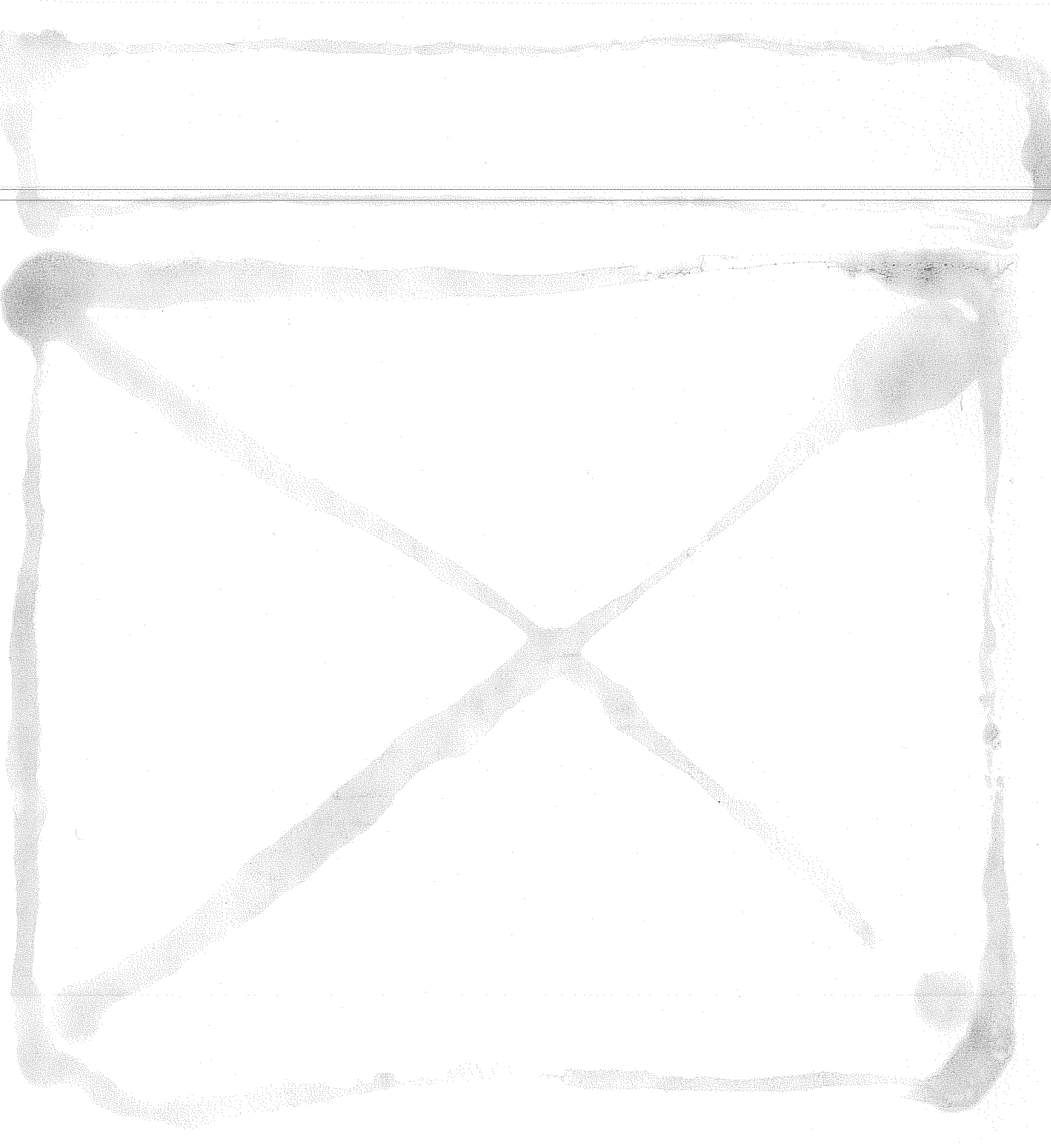
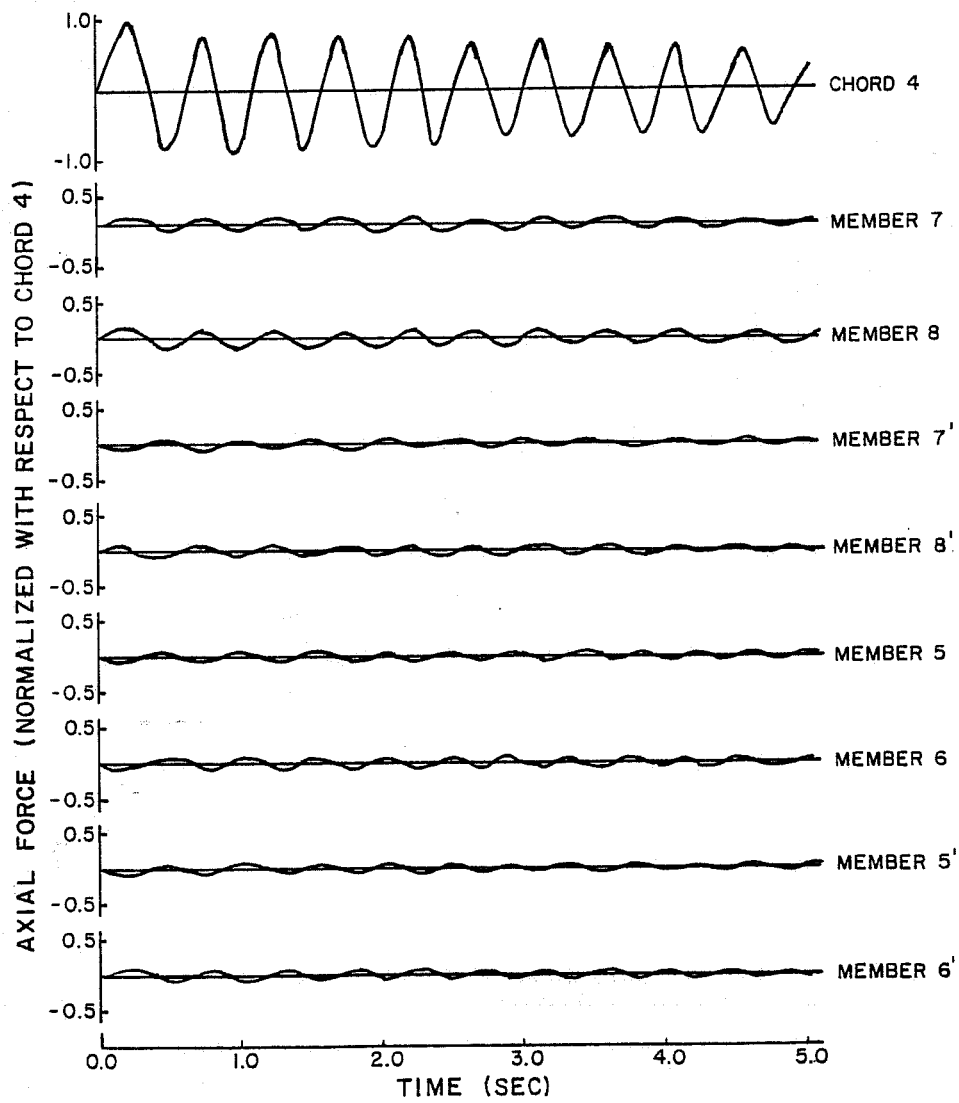


Fig. 4.5 Analytically derived and normalized chord member forces for double cantilever sign



NOTE: POSITIVE VALUES FOR
AXIAL FORCE DENOTE
TENSION



Fig. 4.6 Analytically derived and normalized diagonal member forces for double cantilever sign

Fig. 4.7. This figure shows the analytical solution slightly underestimates the force in the chord after the first peak, when the maxima occur for both plots. The phase difference in the traces is caused by the difference in natural frequency values between the experimental and analytical solutions, as shown in Table 4.1.

The program also calculated dynamic base forces. The maxima for these occurred simultaneously with the axial forces in the chord members of the loaded arm of the sign. These maxima, derived for a p_{\max} due to a 19.2 mph wind speed, are compared with the values obtained from the traces of Fig. 3.1, in Table 4.2.

TABLE 4.2 DOUBLE CANTILEVER EXPERIMENTAL VS ANALYTICAL BASE FORCES

Base Force	Experimental	Analytical
T_b (k-in.)	34.72	34.60
V_y (k)	0.094	0.122
V_x (k)	~ 0	0.012
M_y (k-in.)	-4.98	-8.35
M_x (k-in.)	25.43	34.03

Considering the sensitivity of the base forces to small differences in truss member forces, as was noted for the results shown in Table 3.2, there is good agreement in the results.

Since the points of application and the magnitudes of the maximum applied horizontal loads on the structure were known, it was possible to calculate the maximum base torque DLF. A value of 1.50 was calculated for the analytical model, while a value of 1.51 was calculated for the event associated with Fig. 3.1.

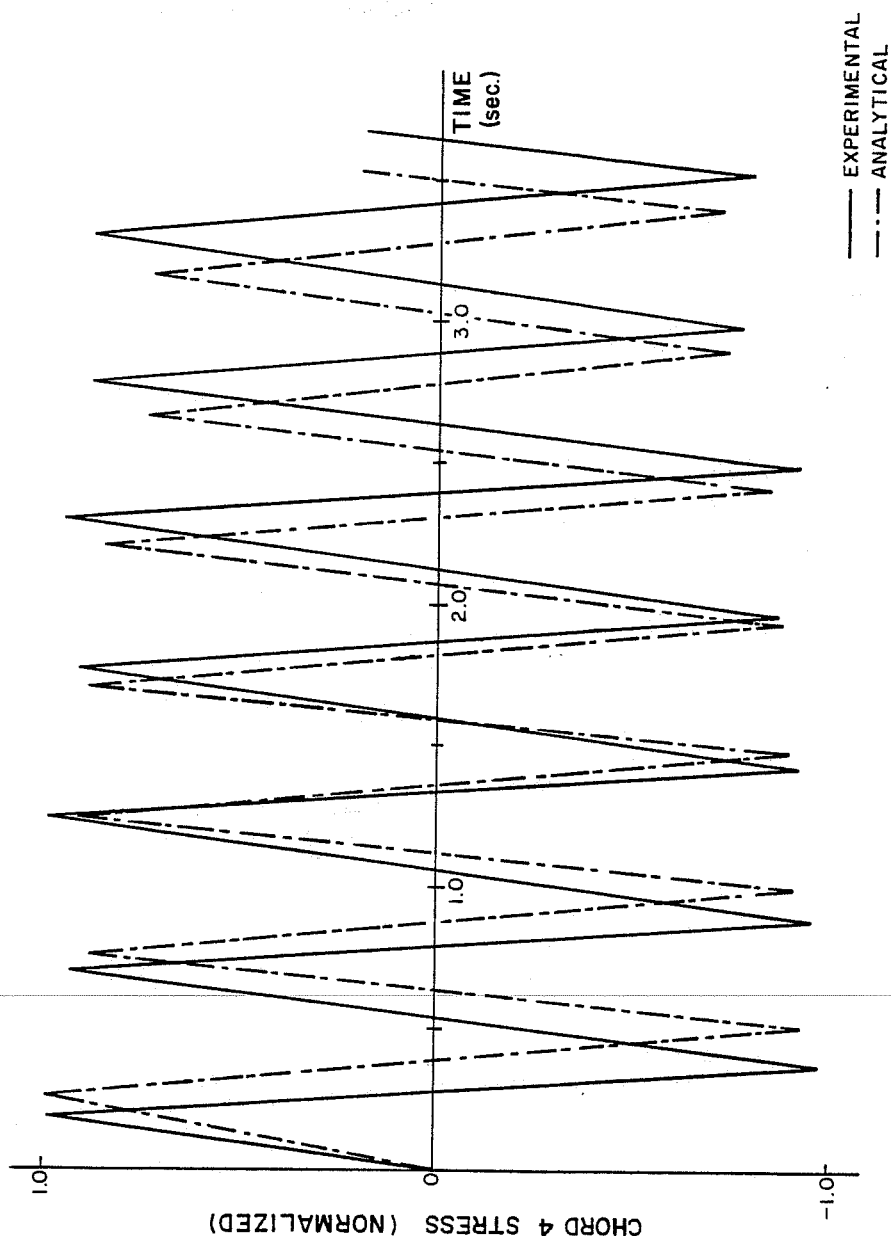


Fig. 4.7 Normalized force outputs for chord member 4 of double cantilever

4.1.3 Single Cantilever. The analytical model for this sign is shown in Fig. 4.4. The program computed eigenvalues and eigenvectors for this system, and close agreement was found between the experimental and analytical frequencies, as given in Table 4.3.

TABLE 4.3 SINGLE CANTILEVER EXPERIMENTAL VS ANALYTICAL NATURAL FREQUENCIES

Mode	Experimental Frequency (cps)	Analytical Frequency (cps)	% Error
First	1.56	1.62	4
Second	1.91	2.09	9

The corresponding eigenvectors indicated that the first mode was primarily a vertical rocking of the truss about the braced-tee support, while the horizontal mode was a horizontal twisting about this support.

The impulse applied on the model was the same used for the double cantilever. The nodal points where the resultant forces were applied and the value of the loading coefficients, α_i , are shown in Fig. 4.4.

The lack of sufficient truck-induced gust loading experimental data for this sign did not allow a valid comparison of the experimental and analytical results. The base forces for both legs of the support were found analytically for a p_{\max} corresponding to a 19.2 mph wind speed. The results are given in Table 4.4.

TABLE 4.4 SINGLE CANTILEVER PREDICTED BASE FORCES

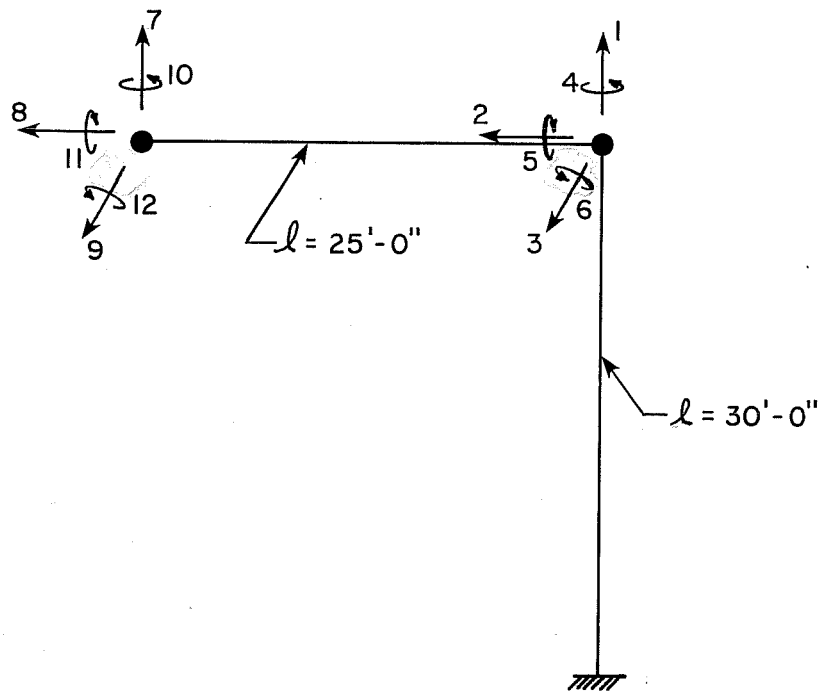
Leg	Torque (kip-in.)	V_y (kips)	V_x (kips)	M_x (kip-in.)	M_y (kip-in.)
Vertical	14.5	0.13	0.02	8.9	0.2
Inclined	6.4	0.13	0.01	9.0	0.2

inclined brace. The other base forces are almost equal in both legs of the support.

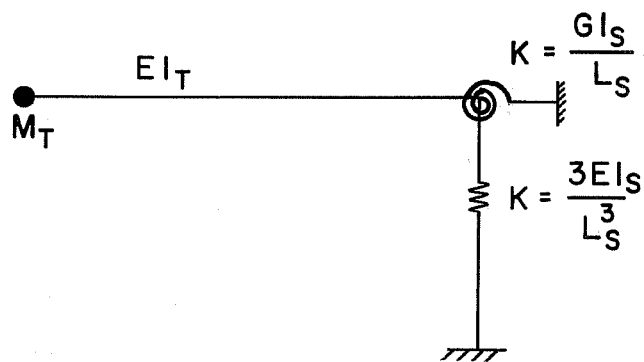
An effort was made to simulate forced vibration of the sign and to determine the reason for the large forces in the bottom chord generated in the experimental forced vibration tests of this sign. A saw-toothed loading of five cycles duration was applied horizontally to the model. The response resulting from the horizontal excitation indicated that the axial forces in the chord members of the bottom chord were approximately three times the magnitude for those of the top chord. This compares favorably with the value of four times found experimentally. The analytical model assumes full compatibility at all joints (no slip). Therefore, the large forces in the bottom chord appear to be due to the shear lag of this deep truss and not due to slippage at the connection of the top chord to the vertical support.

4.2 Preliminary Program

The dynamic response of a single cantilever sign, with dimensions approximately equal to those of the sign instrumented, was investigated using a computer program written by Bohl and the author [4]. The analytical model had 12 DOF, used consistent mass, and is shown in Fig. 4.8(a). Various horizontal impulses were applied to the system and the results indicated that the effects of higher modes on the response of the structure were negligible. Since the model used did not include the individual members found in the actual structure, stress analysis was not possible. However, it was concluded that a simple 3 DOF analysis can adequately predict the response. This is preferred, since it reduces the computations down to hand calculations. This could enable the designer to obtain a preliminary estimate of the importance of dynamic effects on the



(a) 12 DOF MODEL



(b) MODIFIED 3 DOF MODEL

Fig. 4.8 Simplified single cantilever analytical models

sign's response to gusts. The 3 DOF involved are shown in Fig. 4.8(b). This model will be investigated further for other signs in the research study to determine if it can adequately describe a sign's behavior.

C H A P T E R 5

ANALYSIS OF RESULTS

The experimental study indicated that the gust load produced by a truck passing under a sign structure results in a large number of stress cycles. Coupled with high stress ranges, this large number of cycles could cause fatigue problems in the structure. The results indicate, however, that the superstructure is not susceptible to fatigue cracking because of the very low measured stress ranges. The stress range of the anchor bolts used to connect the superstructure to the foundation was not measured directly and required further analysis of the measured results. The calculation of anchor bolt stress ranges for the double cantilever sign will be discussed in this chapter.

5.1 Anchor Bolt Stress Ranges

A sketch of the connection at the base of the vertical support of the double cantilever sign and the forces that act on this connection are shown in Fig. 5.1. These forces are transmitted to the foundation by the anchor bolts. The base forces for the nine events shown in Table 3.2 were used to calculate the anchor bolt stress ranges.

The four 2 in. nominal diameter anchor bolts shown in Fig. 5.1 are subjected to fluctuating direct tension or compression stresses resulting from the biaxial overturning moments M_x and M_y , and a fluctuating bending and shear stress resulting from the resultant shear, V_r . The resultant shear is equal to the vector sum of the portion of the biaxial shears V_x and V_y acting on each

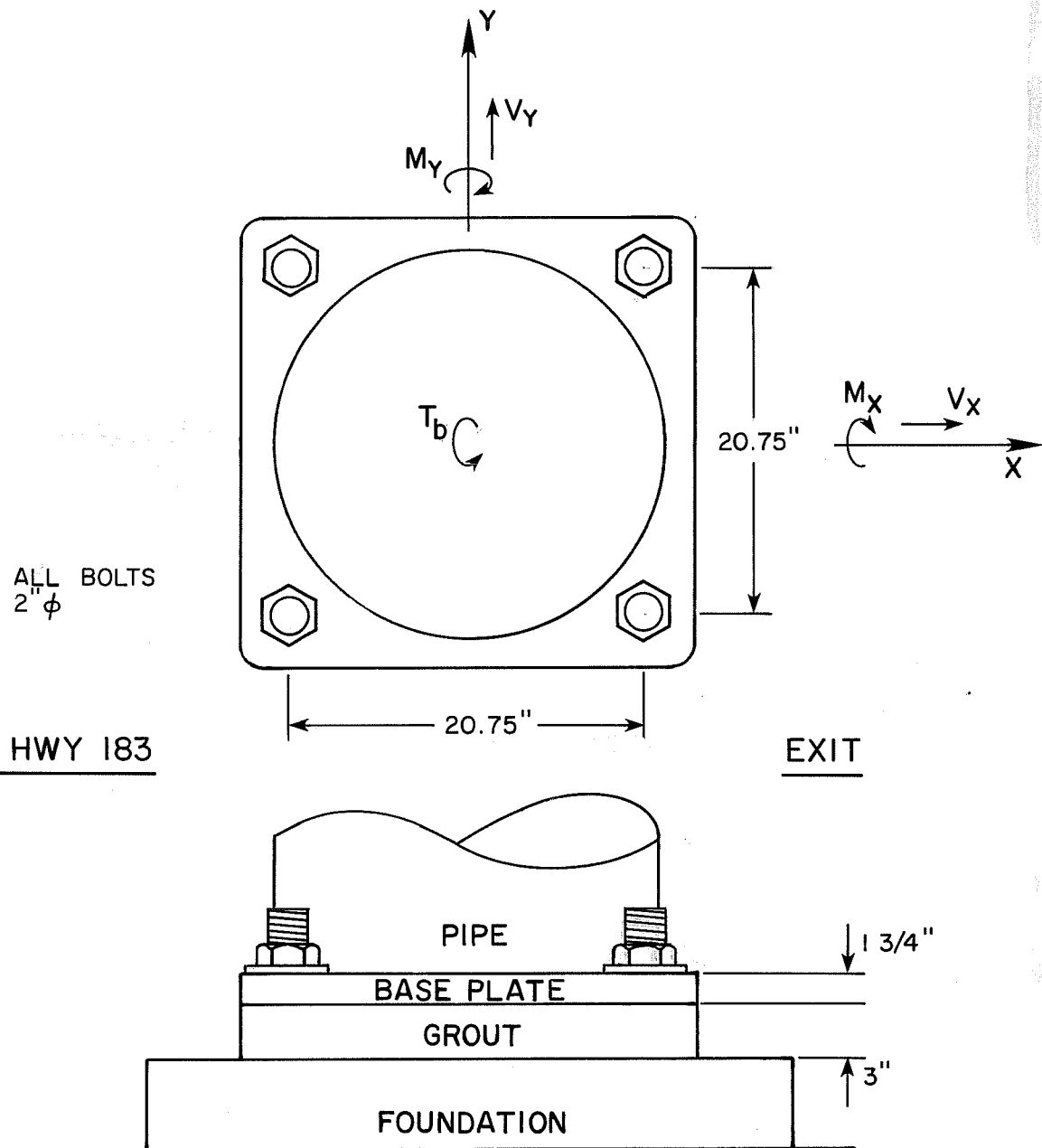


Fig. 5.1 Double cantilever support-to-foundation connection

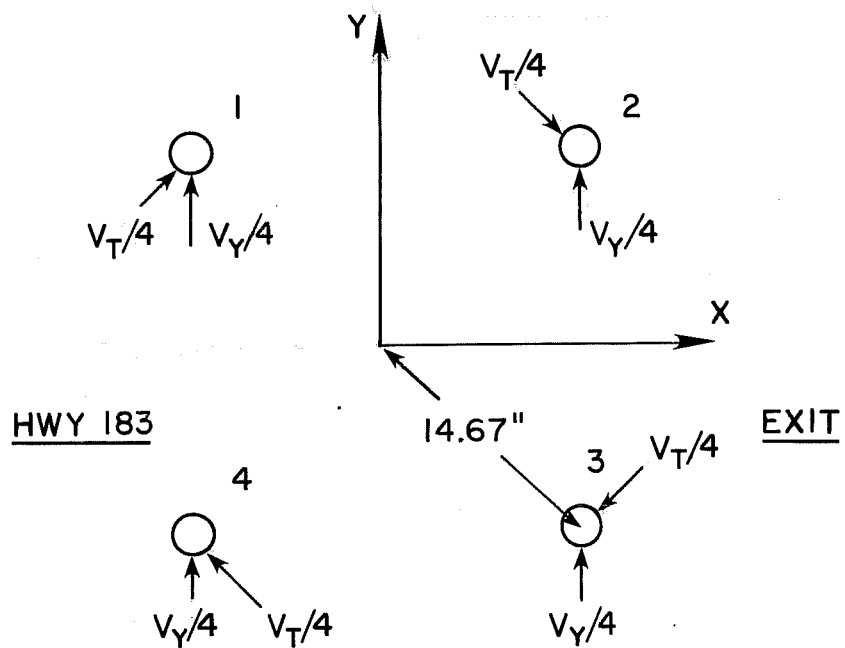
bolt, and the shear, V_T , caused by the base torque. The magnitude of V_x is generally low and was neglected from the calculations that follow. It was assumed that all bolts are capable of carrying shear and that this shear was equal on each of the bolts. This may not be true in the actual sign, due to misaligned and/or oversized holes. Also, the degree to which anchor bolt nuts are tightened affects the mode in which the shear is transferred to the bolt, i.e., whether by bearing or friction. There have been anchor bolt nuts found loose in certain sign structures. The shears $V_T/4$ and $V_y/4$ acting on the anchor bolts are shown schematically in Fig. 5.2(a). The bending moment in the anchor bolt is produced by the resultant shear, V_r , which acts at a length " ℓ " above the foundation. The length " ℓ " was taken as 0.7 times the distance between the bottom of the base plate and the top of the foundation. This value was based on the preliminary results of a study by James [5]. The appropriate value of the length " ℓ " to calculate the moment in the anchor bolt depends on the degree of fixity of the anchor bolt at the foundation and base plate. The actual value of " ℓ " is not known; consequently, the bending stress in the anchor bolt can only be approximated.

The direct tension and compression anchor bolt stresses can be calculated as follows:

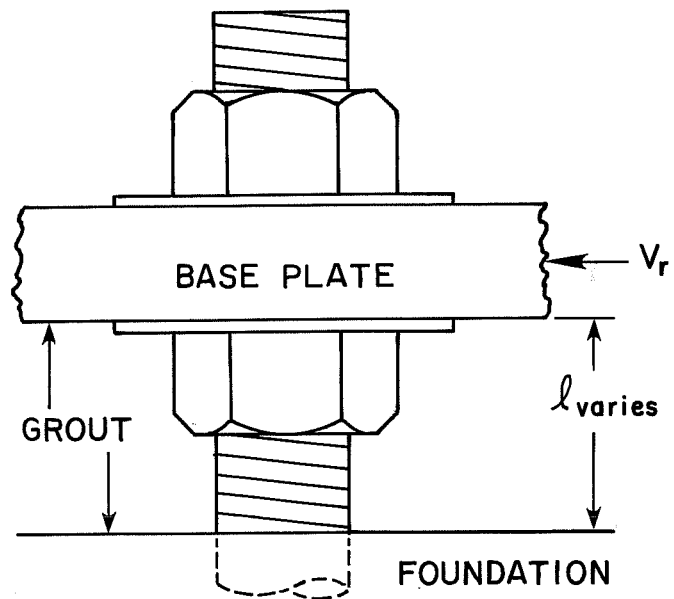
The stress due to M_x is given by the equation

$$\sigma_x = M_x / 4cA_b$$

where σ_x = anchor bolt stress caused by M_x
 M_x = overturning moment parallel to traffic
 c = distance from the x-axis to the centerline of the anchor bolt, 10.375 in.
 A_b = tensile area of the anchor bolt, 2.50 in.²



(a) SHEARS ON BOLT GROUP



(b) RESULTANT SHEAR ON BOLT

Fig. 5.2 Forces acting on anchor bolts

The stress due to M_y is given by the equation

$$\sigma_y = M_y / 4cA_b$$

where σ_y = anchor bolt stress caused by M_y
 M_y = overturning moment in the direction parallel to the length of the truss
 c = 10.375 in.
 A_b = 2.50 in.²

The bending stress in the anchor bolts can be estimated as follows:

The resultant shear is given by the equation

$$\vec{V}_r = \vec{V}_y/4 \text{ and } \vec{V}_T/4$$

where \vec{V}_r = resultant of shears $\vec{V}_y/4$ and $\vec{V}_T/4$

$\vec{V}_y/4$ = shear parallel to traffic

$\vec{V}_T/4$ = shear caused by the base torque and given by the equation

$$V_T/4 = T_b/4\rho$$

where T_b = base torque
 ρ = distance from the center of the base plate to the centerline of the anchor bolts, 14.67 in.

The bending stress is given by the equation

$$\sigma_r = V_r l / S_b$$

where σ_r = bending stress in the anchor bolt
 V_r = resultant due to shears $V_y/4$ and $V_T/4$
 l = 0.7 times the distance from the bottom of the base plate to the top of the foundation
 S_b = section modulus of the anchor bolt, 0.556 in.³ based on tensile stress area diameter, 1.783 in.

Example 5.1: The stress ranges for anchor bolt 4 of the double cantilever sign during event 1 of Table 3.2 are

$$\sigma_x = \frac{25.43}{4(10.375)2.50} = 0.25 \text{ ksi, tension}$$

$$\sigma_y = \frac{4.98}{4(10.375)2.50} = 0.05 \text{ ksi, tension}$$

$$V_T = \frac{34.72}{4(14.67)} = 0.592 \text{ kips}$$

$$V_r = [(0.592 \cos 45^\circ) + (\frac{0.094}{4} + 0.592 \sin 45^\circ)^2]^{1/2}$$

$$V_r = 0.609 \text{ kips}$$

and
$$\sigma_r = \frac{0.609(0.7)3}{0.556} = 2.30 \text{ ksi}$$

These results can be combined by calculating the corresponding total stress range assuming that the stresses are in phase.

$$S_R = 2(0.25 + 0.05 + 2.30) = 5.20 \text{ ksi}$$

It should be noted that this stress range corresponds to event 1 during which a box-type truck produced the maximum measured response of the structure.

The anchor bolt stresses associated with the base forces shown in Table 3.2 resulted in the values given in Table 5.1. These values indicate that the predominant stress in the anchor bolts is the bending stress, σ_r , caused by the resultant shear, V_r .

5.2 Fatigue Analysis

To design against fatigue of a structure's component, the engineer must estimate the stress range that the component is subjected to and the total number of cycles at this stress range expected over the lifetime of the structure. By entering this

TABLE 5.1 MAXIMUM ANCHOR BOLT STRESSES
ASSOCIATED WITH TABLE 3.2

Event	σ_r (ksi)	σ_x (ksi)	σ_y (ksi)	S_r (ksi)
1	2.30	0.25	0.05	5.20
2	1.89	0.21	0.11	4.42
3	1.79	0.21	0.08	4.16
4	1.78	0.21	0.10	4.18
5	1.68	0.18	0.02	3.76
6	1.55	0.17	0.10	3.64
7	1.54	0.19	0.11	3.68
8	1.37	0.20	0.10	3.34
9	1.28	0.17	0.01	2.92

stress range in a log stress range versus log number of cycles curve, an S-N curve, for the component, the engineer can estimate the total number of cycles at this stress range to cause failure. If the total number of cycles the component is subjected to is less than this value, the design would be satisfactory.

The values of stress shown in Table 5.1 indicated that the bending moment caused by the base shear resultant, V_r , on the anchor bolt produced the highest anchor bolt stresses. The major components of this shear resultant are the shear due to the base torque and the shear, V_y . Consequently, the stress range, S_r , in the anchor bolt is proportional to the base torque range, T_R , and to the shear range, $V_{R,y}$. A linear relationship between T_R and $V_{R,y}$ would be expected for a simple static loading with $T_R = LV_R$, where L is a length corresponding to the point of application of a statically equivalent horizontal load on the sign. A plot of T_R versus $V_{R,y}$ based on the results shown in Tables 3.2 and 4.2 was constructed and is shown in

Fig. 5.3. An apparent linear relationship between T_R and V_R is evident. A linear least squares fit of the data points resulted in the line shown in the figure and given by the equation

$$T_R = 0.318 + 334 V_{R,y}$$

where T_R is in kip-in. and $V_{R,y}$ is in kips. Consequently, the resultant base shear, V_r , if either T_R or $V_{R,y}$ is known.

The experimental results indicated that the stress ranges in the structure caused by the passing of a single truck are not constant and decay with time from the initial maximum stress range. Also, the maximum stress range, $S_{R \max}$, for each truck passing under the sign was different. A procedure was developed to determine a representative or effective stress range, S_{Re} , to correlate these results based on the T_R .

The number and magnitudes of torque range cycles for the double cantilever sign produced by a single truck was estimated using the equation for damped free vibration.

$$T_{R_i} = T_{R \max} e^{-\xi \omega t}$$

where T_{R_i} = torque range at time, t

$T_{R \max}$ = maximum torque range, taken as $2 \times T_b$ given in Table 3.2

ξ = damping ratio, taken as 0.69 percent

ω = circular frequency, taken as 12.6 rad/sec

t = time at intervals of $T/2 + jT$ sec, where T = natural period, 0.5 sec and $j = 0, 1, 2, \dots, n$

Since T_R was generated primarily from the second or horizontal mode, the second mode circular frequency and damping ratio values were used.

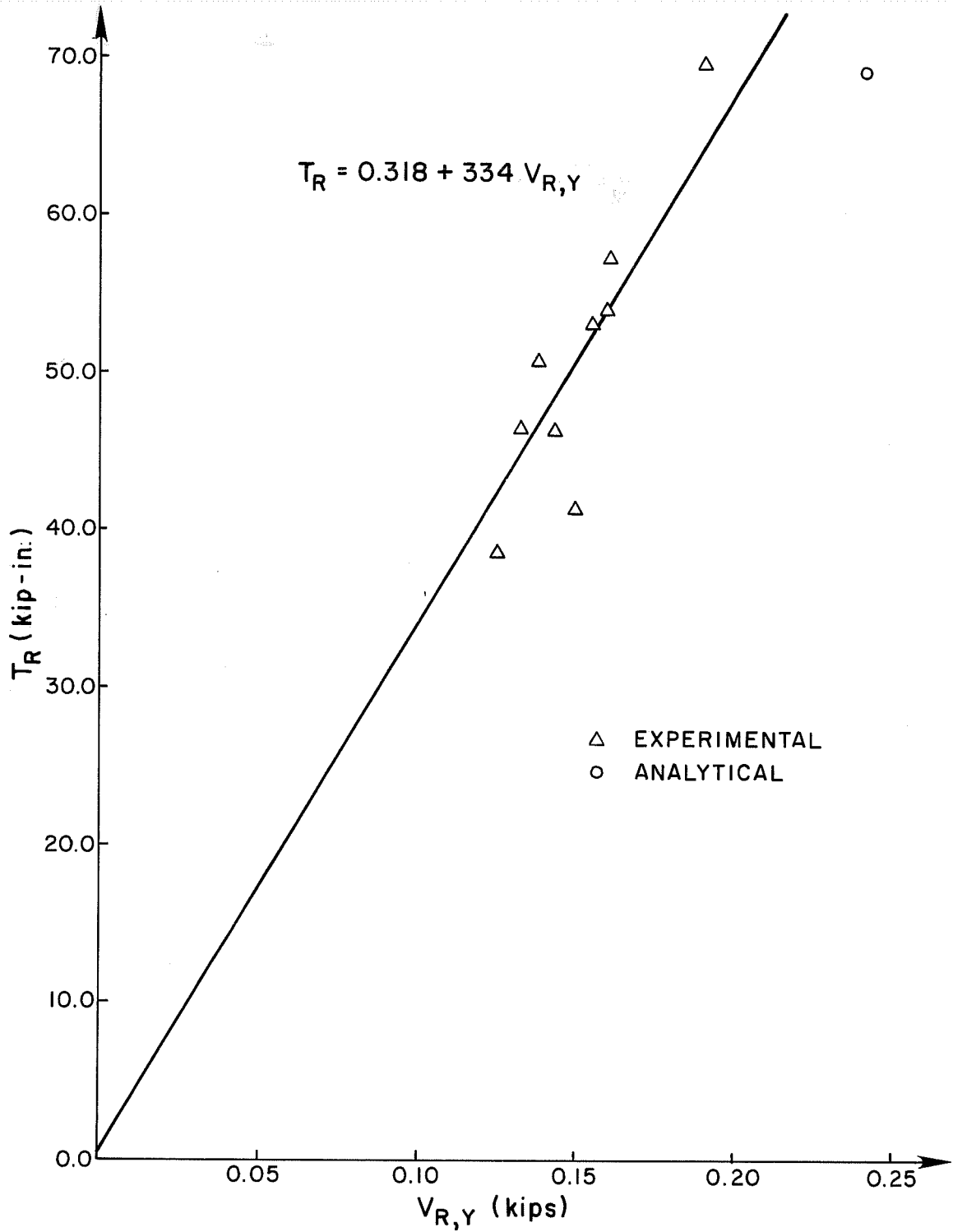


Fig. 5.3 Base torque range, T_R , as a function of base shear range, $V_{R,y}$

The equation indicated that approximately 33 cycles were necessary for $T_{R,i}$ to reach a value of $0.25T_{R \max}$. This value resulted in a reasonable number of significant torque ranges to be considered in the analysis. An effective torque range, T_{R_e} , was then calculated for the base torque values given in Table 3.2 using Miner's Law. The equation for T_{R_e} , given in an AISC publication by Fisher [4], is

$$T_{R_e} = [\sum Y_i (T_{R_i})^3]^{1/3}$$

where T_{R_e} = effective base torque range

$$Y_i = 1/\text{total number of cycles} = 1/9 \times 35$$

T_{R_i} = base torque range at time t

The resulting effective base torque range for the nine events shown in Table 3.2 had a value of 32.0 kip-in. A histogram of total number of cycles versus the torque range, T_{R_i} , was constructed and is shown in Fig. 5.4. Using the graph shown in Fig. 5.3, a T_{R_e} of 32.0 kip-in. corresponds to a V_{R,y_e} of 0.095 kips. Using the procedure to calculate anchor bolt stresses, these values result in a S_{R_e} of approximately 2.5 ksi in anchor bolt 4.

The total number of cycles at this S_{R_e} would be estimated by multiplying the total number of box-type trucks expected on the highway during the design life of the sign by 33. The cycles corresponding to failure of the anchor bolt are found by entering a S-N curve for the anchor bolt at the level of S_{R_e} calculated and finding the number corresponding to failure at the level of S_{R_e} . If the number of cycles produced by the trucks is less than that corresponding to failure at the calculated value of S_{R_e} , the anchor bolt would be adequate.

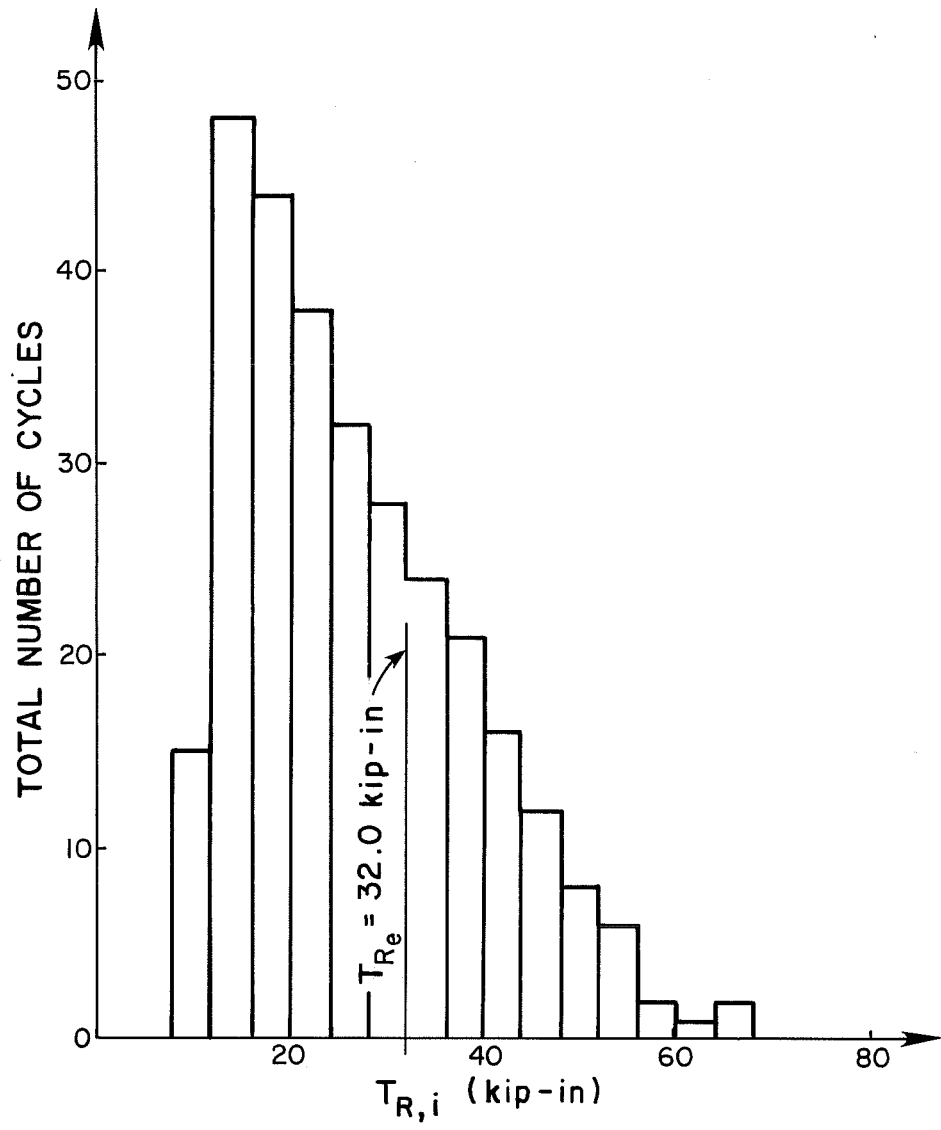


Fig. 5.4 Histogram of torque range, T_R

An anchor bolt stress analysis for the single cantilever was made based on the predicted base forces given in Table 4.4. Calculations were made for the four 2-3/4 in. diameter anchor bolts of the vertical leg base plate. The results indicated a maximum stress range, S_R , of 1.29 ksi for the loading assumed in the analytical procedure.

CHAPTER 6

CONCLUSIONS AND RECOMMENDATIONS

This study consisted of instrumentation of a single and a double cantilever highway sign structure and an analytical analysis of both signs. The dynamic response of these structures to actual and simulated truck-induced gust loadings and to forced vibration tests was investigated and led to the following conclusions:

(1) Good agreement was found between the experimental and analytical first and second mode natural frequency values.

(2) For both signs the first mode was a vertical rocking of the truss about the pipe support while the second mode was a horizontal movement of the sign with the truss rotation about the support.

(3) Beating occurred in the double cantilever and was attributed to a combination of the responses of the first and second modes, whose periods were very close to each other.

(4) The damping ratio for both signs was very low, less than 1 percent of critical, and resulted in a large number of stress cycles produced following a truck passage under the sign face.

(5) The superstructure stresses caused by truck-induced gusts are low and present no fatigue problem.

(6) Box-type trucks produced the highest superstructure stresses measured.

(7) The maximum anchor bolt stresses are caused by the shear resulting from the base torque.

(8) A loading function was developed which simulated the gust produced by a truck passing under a sign.

(9) Good agreement was found between the experimental and analytical results for the stresses in the chord members of the loaded arm of the double cantilever.

(10) A procedure for calculations of a fatigue analysis of the anchor bolts was presented.

Additional field study should be conducted, particularly on single cantilever sign structures with large traffic volumes. The possibility of aerodynamic resistance of the unloaded arm of the double cantilever requires further examination. Refinement of the analytical procedure is recommended. The development of a simple procedure to determine base forces would be advantageous to the design engineer.

B I B L I O G R A P H Y

1. Clough, Ray W., and Penzien, Joseph, Dynamics of Structures, McGraw-Hill Book Company, Inc., New York, 1975.
2. Bathe, Klaus-Jürgen, Wilson, Edward, and Peterson, Fred, SAP IV Structural Analysis Program," University of California at Berkeley, April 1974.
3. Kyropoulos, Peter, "Truck Aerodynamics," SAE Transactions, 1962, p. 307.
4. Bohl, Alfredo, and Cocavessis, Nicolas, "Dynamic Analysis of Single Cantilever Sign Structure," computer program developed at The University of Texas at Austin, April 1977.
5. James, Billy D., Oral conversation concerning M.S. thesis in progress at The University of Texas at Austin, November 1977.

V I T A

Nicolas Steven Cocavessis was born on July 7, 1953, in Alexandria, U.A.R., to Steven and Alexandra Cocavessis. After graduating from the American Community School in Athens, Greece, he attended the University of Arizona where he received a Bachelor of Science in May 1976. He enrolled in the Graduate School of The University of Texas at Austin in September 1976.

Permanent address: 3440 North Winslow Drive
Tucson, Arizona 85715

This thesis was typed by Maxine R. DeButts.